

Meta-learning framework with applications to zero-shot time-series forecasting

Boris N. Oreshkin¹, Dmitri Carpv¹, Nicolas Chapados¹, Yoshua Bengio²

¹Element AI, ²Mila
boris.oreshkin@gmail.com

Abstract

Can meta-learning discover generic ways of processing time-series (TS) from a diverse dataset so as to greatly improve generalization on new TS coming from different datasets? This work provides positive evidence to this using a broad meta-learning framework which we show subsumes many existing meta-learning algorithms. Our theoretical analysis suggests that residual connections act as a meta-learning adaptation mechanism, generating a subset of task-specific parameters based on a given TS input, thus gradually expanding the expressive power of the architecture on-the-fly. The same mechanism is shown via linearization analysis to have the interpretation of a sequential update of the final linear layer. Our empirical results on a wide range of data emphasize the importance of the identified meta-learning mechanisms for successful zero-shot univariate forecasting, suggesting that it is viable to train a neural network on a source TS dataset and deploy it on a different target TS dataset without retraining, resulting in performance that is at least as good as that of state-of-practice univariate forecasting models.

1 Introduction

Time series (TS) forecasting is both a fundamental scientific problem and one of great practical importance; unsurprisingly, forecasting methods have a long history that can be traced back to the very origins of human civilization (Neale 1985), modern science (Gauss 1809) and have consistently attracted considerable research attention (Yule 1927; Walker 1931; Holt 1957; Winters 1960; Engle 1982; Sezer, Gudelek, and Ozbayoglu 2019). The progress made in univariate forecasting in the past four decades is well reflected in the results and methods considered in associated competitions over that period (Makridakis et al. 1982, 1993; Makridakis and Hibon 2000; Athanasopoulos et al. 2011; Makridakis, Spiliotis, and Assimakopoulos 2018a). In recent years, growing evidence has started to emerge suggesting that some machine learning approaches could improve on classical approaches for forecasting tasks, in contrast to some earlier assessments (Makridakis, Spiliotis, and Assimakopoulos 2018b). For example, the winner of the 2018 M4 competition (Makridakis, Spiliotis, and Assimakopoulos 2018a) was a neural network designed by Smyl (2020).

On the practical side, the deployment of deep neural time-series models is challenged by the cold start problem. Before

a *tabula rasa* deep neural network provides a useful forecasting output, it should be trained on a large problem-specific time-series dataset. For early adopters, this often implies data collection efforts, changing data handling practices and even changing the existing IT infrastructures on a large scale. In contrast, advanced statistical models can be deployed with significantly less effort as they estimate their parameters on single time series at a time. In this paper we address the problem of reducing the entry cost of deep neural networks in the industrial practice of TS forecasting. We show that it is viable to train a neural network model on a diversified source dataset and deploy it on a target dataset in a *zero-shot regime*, i.e. without explicit retraining on that target data, resulting in performance that is at least as good as that of advanced statistical models tailored to the target dataset.

Addressing this practical problem provides clues to fundamental questions. Can we learn something general about forecasting and transfer this knowledge across datasets? If so, what kind of mechanisms could facilitate this? The ability to learn and transfer representations across tasks via task adaptation is an advantage of meta-learning (Raghu et al. 2019). We propose here a broad theoretical framework for meta-learning that encompasses several existing meta-learning algorithms. We further show that a recent successful model, N-BEATS (Oreshkin et al. 2020), fits this framework. We identify internal meta-learning adaptation mechanisms that generate new parameters on-the-fly, specific to a given TS, iteratively extending the architecture’s expressive power. We empirically confirm that meta-learning mechanisms are key to improving zero-shot TS forecasting performance, and demonstrate results on a wide range of datasets.

1.1 Background

The univariate point forecasting problem in discrete time is formulated given a length- H forecast horizon and a length- T observed series history $[y_1, \dots, y_T] \in \mathbb{R}^T$. The task is to predict the vector of future values $\mathbf{y} \in \mathbb{R}^H = [y_{T+1}, y_{T+2}, \dots, y_{T+H}]$. For simplicity, we will later consider a *lookback window* of length $t \leq T$ ending with the last observed value y_T to serve as model input, and denoted $\mathbf{x} \in \mathbb{R}^t = [y_{T-t+1}, \dots, y_T]$. We denote $\hat{\mathbf{y}}$ the point forecast of \mathbf{y} . Its accuracy can be evaluated with SMAPE, the symmetric mean absolute percentage error (Makridakis, Spiliotis,

and Assimakopoulos 2018a),

$$\text{sMAPE} = \frac{200}{H} \sum_{i=1}^H \frac{|y_{T+i} - \hat{y}_{T+i}|}{|y_{T+i}| + |\hat{y}_{T+i}|}. \quad (1)$$

Other quality metrics (e.g. MAPE, MASE, OWA, ND) are possible and are defined in Appendix A.

Meta-learning or *learning-to-learn* (Harlow 1949; Schmidhuber 1987; Bengio, Bengio, and Cloutier 1991) is hypothesized to be necessary for intelligent machines (Lake et al. 2017). The ability to meta-learn is usually linked to being able to (i) accumulate knowledge across different tasks (*i.e. transfer learning, multi-task learning*) and (ii) quickly adapt the accumulated knowledge to the new task (*task adaptation*) (Ravi and Larochelle 2016; Lake et al. 2017; Bengio et al. 1992).

For univariate point point forecasting, the **N-BEATS** algorithm has demonstrated outstanding performance on several competition benchmarks (Oreshkin et al. 2020). The model consists of a total of L blocks connected using a doubly residual architecture. Block ℓ has input \mathbf{x}_ℓ and produces two outputs: the *backcast* $\hat{\mathbf{x}}_\ell$ and the *partial forecast* $\hat{\mathbf{y}}_\ell$. For the first block we define $\mathbf{x}_1 \equiv \mathbf{x}$, where \mathbf{x} is assumed to be the model-level input from now on. We define the k -th fully-connected layer in the ℓ -th block, having ReLU non-linearity (Nair and Hinton 2010; Glorot, Bordes, and Bengio 2011), weight matrix \mathbf{W}_k , bias vector \mathbf{b}_k and input $\mathbf{h}_{\ell,k-1}$, as $\text{FC}_k(\mathbf{h}_{\ell,k-1}) \equiv \text{ReLU}(\mathbf{W}_k \mathbf{h}_{\ell,k-1} + \mathbf{b}_k)$. Note that we focus on the configuration that shares all learnable parameters across blocks. With this notation, one block of N-BEATS is described as:

$$\begin{aligned} \mathbf{h}_{\ell,1} &= \text{FC}_1(\mathbf{x}_\ell), \quad \mathbf{h}_{\ell,k} = \text{FC}_k(\mathbf{h}_{\ell,k-1}), \quad k = 2 \dots K; \\ \hat{\mathbf{x}}_\ell &= \mathbf{Q}\mathbf{h}_{\ell,K}, \quad \hat{\mathbf{y}}_\ell = \mathbf{G}\mathbf{h}_{\ell,K}, \end{aligned} \quad (2)$$

where \mathbf{Q} and \mathbf{G} are linear operators. The N-BEATS parameters included in the FC and linear layers are learned by minimizing a suitable loss function (*e.g.* SMAPE defined in (1)) across multiple TS. Finally, the doubly residual architecture is described by the following recursion (recalling that $\mathbf{x}_1 \equiv \mathbf{x}$):

$$\mathbf{x}_\ell = \mathbf{x}_{\ell-1} - \hat{\mathbf{x}}_{\ell-1}, \quad \hat{\mathbf{y}} = \sum_{\ell=1}^L \hat{\mathbf{y}}_\ell. \quad (3)$$

1.2 Related Work

From a high-level perspective, there are many links with classical TS modeling: a human-specified classical model is typically designed to generalize well on unseen TS, while we propose to automate that process. The classical models include exponential smoothing with and without seasonal effects (Holt 1957, 2004; Winters 1960), multi-trace exponential smoothing approaches, *e.g.* Theta and its variants (Assimakopoulos and Nikolopoulos 2000; Fiorucci et al. 2016; Spiliotis, Assimakopoulos, and Nikolopoulos 2019). Finally, the state space modeling approach encapsulates most of the above in addition to auto-ARIMA and GARCH (Engle 1982; see Hyndman and Khandakar (2008) for an overview). The state-space approach has also been underlying significant amounts of research in the neural TS modeling (Salinas et al. 2019; Wang et al. 2019; Rangapuram et al. 2018). However,

those models have not been considered in the zero-shot scenario. In this work we focus on studying the importance of meta-learning for successful zero-shot forecasting. The foundations of meta-learning have been developed by Schmidhuber (1987); Bengio, Bengio, and Cloutier (1991) among others. More recently, meta-learning research has been expanding, mostly outside of the TS forecasting domain (Ravi and Larochelle 2016; Finn, Abbeel, and Levine 2017; Snell, Swersky, and Zemel 2017; Vinyals et al. 2016; Rusu et al. 2019). In the TS domain, meta-learning has manifested itself via neural models trained over a collection of TS (Smyl 2020; Oreshkin et al. 2020) or via a model trained to predict weights combining outputs of several classical forecasting algorithms (Montero-Manso et al. 2020). Successful application of a neural TS forecasting model trained on a source dataset and fine-tuned on the target dataset was demonstrated by Hooshmand and Sharma (2019); Ribeiro et al. (2018) as well as in the context of TS classification by Fawaz et al. (2018). Unlike those, we focus on the zero-shot scenario and address the cold start problem.

1.3 Summary of Contributions

Meta-learning framework: we define a generalized meta-learning framework with associated equations, and recast within it many existing meta-learning algorithms. We show that N-BEATS follows the same equations. In particular, we show that each block within N-BEATS corresponds to an inner meta-learning loop generating additional effective parameters, despite all blocks sharing their (train-time, static) network parameters and N-BEATS not performing any gradient steps at inference time. Building on this, we empirically establish that the meta-learning component is important for zero-shot generalization in univariate time-series forecasting.

Zero-shot univariate time-series forecasting task: we define a novel machine learning forecasting task and make its dataset loaders and evaluation code public, including a new large-scale dataset (FRED) with 290k TS.

The feasibility and viability of the zero-shot TS forecasting: we empirically show, for the first time, that zero-shot time series forecasting is amenable to deep learning. We further show that on a diverse range of univariate time series forecasting benchmarks, N-BEATS’ zero-shot forecasting accuracy nears the state of the art, making a strong baseline model for a wide variety of application areas.

2 Meta-learning Framework

A meta-learning procedure can generally be viewed at two levels: the *inner loop* and the *outer loop*. The inner training loop operates within an individual “meta-example” or task \mathcal{T} (fast learning loop improving over current \mathcal{T}) and the outer loop operates across tasks (slow learning loop). A task \mathcal{T} includes task training data $\mathcal{D}_{\mathcal{T}}^{tr}$ and task validation data $\mathcal{D}_{\mathcal{T}}^{val}$, both optionally involving inputs, targets and a task-specific loss: $\mathcal{D}_{\mathcal{T}}^{tr} = \{\mathcal{X}_{\mathcal{T}}^{tr}, \mathcal{Y}_{\mathcal{T}}^{tr}, \mathcal{L}_{\mathcal{T}}\}$, $\mathcal{D}_{\mathcal{T}}^{val} = \{\mathcal{X}_{\mathcal{T}}^{val}, \mathcal{Y}_{\mathcal{T}}^{val}, \mathcal{L}_{\mathcal{T}}\}$. Accordingly, a meta-learning set-up can be defined by assuming a distribution $p(\mathcal{T})$ over tasks, a predictor $\mathcal{P}_{\theta, \mathbf{w}}$ and a meta-learner with meta-parameters ϕ . We allow a subset of predictor’s parameters denoted \mathbf{w} to belong to meta-parameters

φ and hence not to be task adaptive. The objective is to design a meta-learner that can generalize well on a new task by appropriately choosing the predictor’s task adaptive parameters θ after observing $\mathcal{D}_{\mathcal{T}_i}^r$. The meta-learner is trained to do so by being exposed to many tasks in a training dataset $\{\mathcal{T}_i^{rain}\}$ sampled from $p(\mathcal{T})$. For each training task \mathcal{T}_i^{rain} , the meta-learner is requested to produce the solution to the task in the form of $\mathcal{P}_{\theta, \mathbf{w}} : \mathcal{X}_{\mathcal{T}_i}^{val} \mapsto \hat{\mathcal{Y}}_{\mathcal{T}_i}^{val}$ and the meta-learner meta-parameters φ are optimized across many tasks based on validation data and loss functions supplied with the tasks. Training on multiple tasks enables the meta-learner to produce solutions \mathcal{P}_{θ} that generalize well on a set of unseen tasks $\{\mathcal{T}_i^{est}\}$ sampled from $p(\mathcal{T})$.

Consequently, the meta-learning procedure has three distinct ingredients: (i) meta-parameters $\varphi = (\mathbf{t}_0, \mathbf{w}, \mathbf{u})$, (ii) initialization function $\mathcal{J}_{\mathbf{t}_0}$ and (iii) update function $\mathcal{U}_{\mathbf{u}}$. The **meta-learner’s meta-parameters** φ include the meta-parameters of the meta-initialization function, \mathbf{t}_0 , the meta-parameters of the predictor shared across tasks, \mathbf{w} , and the meta-parameters of the update function, \mathbf{u} . The **meta-initialization function** $\mathcal{J}_{\mathbf{t}_0}(\mathcal{D}_{\mathcal{T}_i}^r, \mathbf{c}_{\mathcal{T}_i})$ defines the initial values of parameters θ for a given task \mathcal{T}_i based on its meta-initialization parameters \mathbf{t}_0 , task training dataset $\mathcal{D}_{\mathcal{T}_i}^r$ and task meta-data $\mathbf{c}_{\mathcal{T}_i}$. Task meta-data may have, for example, a form of task ID or a textual task description. The **update function** $\mathcal{U}_{\mathbf{u}}(\theta_{\ell-1}, \mathcal{D}_{\mathcal{T}_i}^r)$ is parameterized with update meta-parameters \mathbf{u} . It defines an iterated update to predictor parameters θ at iteration ℓ based on their previous value and the task training set $\mathcal{D}_{\mathcal{T}_i}^r$. The initialization and update functions produce a sequence of predictor parameters, which we compactly write as $\theta_{0:\ell} \equiv \{\theta_0, \dots, \theta_{\ell-1}, \theta_{\ell}\}$. We let the final predictor be a function of the whole sequence of parameters, written compactly as $\mathcal{P}_{\theta_{0:\ell}, \mathbf{w}}$. One implementation of such general function could be a Bayesian ensemble or a weighted sum, for example: $\mathcal{P}_{\theta_{0:\ell}, \mathbf{w}}(\cdot) = \sum_{j=0}^{\ell} \omega_j \mathcal{P}_{\theta_j, \mathbf{w}}(\cdot)$. If we set $\omega_j = 1$ iff $j = \ell$ and 0 otherwise, then we get the more common situation $\mathcal{P}_{\theta_{0:\ell}, \mathbf{w}}(\cdot) \equiv \mathcal{P}_{\theta_{\ell}, \mathbf{w}}(\cdot)$.

The meta-parameters φ are updated in the outer meta-learning loop so as to obtain good generalization in the inner loop, *i.e.*, by minimizing the expected validation loss $\mathbb{E}_{\mathcal{T}_i} \mathcal{L}_{\mathcal{T}_i}(\hat{\mathcal{Y}}_{\mathcal{T}_i}^{val}, \mathcal{Y}_{\mathcal{T}_i}^{val})$ mapping the ground truth and estimated outputs into the value that quantifies the generalization performance across tasks. This meta-learning framework is succinctly described by the following set of equations:

$$\begin{aligned} \text{Parameters: } & \theta; \quad \text{Meta-parameters: } \varphi = (\mathbf{t}_0, \mathbf{w}, \mathbf{u}) \\ \text{Inner Loop: } & \theta_0 \leftarrow \mathcal{J}_{\mathbf{t}_0}(\mathcal{D}_{\mathcal{T}_i}^r, \mathbf{c}_{\mathcal{T}_i}) \\ & \theta_{\ell} \leftarrow \mathcal{U}_{\mathbf{u}}(\theta_{\ell-1}, \mathcal{D}_{\mathcal{T}_i}^r), \forall \ell > 0 \end{aligned} \quad (4)$$

$$\begin{aligned} \text{Prediction at } \mathbf{x} : & \mathcal{P}_{\theta_{0:\ell}, \mathbf{w}}(\mathbf{x}) \\ \text{Outer Loop: } & \varphi \leftarrow \varphi - \eta \nabla_{\varphi} \mathcal{L}_{\mathcal{T}_i}[\mathcal{P}_{\theta_{0:\ell}, \mathbf{w}}(\mathcal{X}_{\mathcal{T}_i}^{val}), \mathcal{Y}_{\mathcal{T}_i}^{val}]. \end{aligned} \quad (5)$$

2.1 Meta-learning and time-series forecasting

In the previous section we laid out a unifying framework for meta-learning. How is it connected to the time-series forecasting task? We believe that this question is best answered by answering questions “why the classical statistical

time-series forecasting models such as ARIMA and ETS are not doing meta-learning?” and “what does the meta-learning component offer when it is part of a time-series forecasting algorithm?”. The first question can be answered by considering the fact that the classical statistical time-series models produce a forecast by estimating their parameters from the history of the target time series using a predefined fixed set of rules, for example, given a model selection and the maximum likelihood parameter estimator for it. Therefore, in terms of our meta-learning framework, a classical time-series model executes only the inner loop (model parameter estimation) encapsulated in equation (4) with a fixed predictor function (e.g. ETS). The outer loop in this case is irrelevant, as a human analyst defines what equation (4) is doing, based on experience (for example, “for most slow varying time-series with trend, no seasonality and white Gaussian noise residuals, ETS with Gaussian maximum likelihood parameter estimator will probably work well”). The second question can be answered considering that meta-learning based time-series forecasting algorithm replaces the predefined fixed set of rules for model parameter estimation with a learnable parameter estimation strategy. The learnable parameter estimation strategy is trained using outer loop equation (5) by adjusting the strategy such that it is able to produce parameter estimates that generalize well over multiple time-series. It is assumed that there exists a dataset that is representative of the forecasting tasks that will be handled at inference time. Thus the main advantage of meta-learning based forecasting approaches is that they enable learning a data-driven model (predictor) parameter estimation rule that can be optimized for a particular set of forecasting tasks. On top of that, a meta-learning approach allows for a general learnable predictor in equation (4) that can be optimized for a given forecasting task. So both predictor (model) and its parameter estimation procedure can be jointly learned for a forecasting task represented by available data. Empirically, we show that this elegant theoretical concept works effectively across multiple datasets and across multiple forecasting tasks (e.g. forecasting yearly, monthly or hourly time-series) and even across very loosely related tasks (for example, forecasting hourly electricity demand after training on a monthly economic data after appropriate time scale normalization).

2.2 Expressing Existing Meta-Learning Algorithms in the Proposed Framework

To further illustrate the generality of the proposed framework, we next show how to cast existing meta-learning algorithms within it, before turning to N-BEATS.

MAML and related approaches (Finn, Abbeel, and Levine 2017; Li et al. 2017; Raghu et al. 2019) can be derived from (4) and (5) by (i) setting \mathcal{J} to be the identity map that copies \mathbf{t}_0 into θ , (ii) setting \mathcal{U} to be the SGD gradient update: $\mathcal{U}_{\mathbf{u}}(\theta, \mathcal{D}_{\mathcal{T}_i}^r) = \theta - \alpha \nabla_{\theta} \mathcal{L}_{\mathcal{T}_i}(\mathcal{P}_{\theta, \mathbf{w}}(\mathcal{X}_{\mathcal{T}_i}^r), \mathcal{Y}_{\mathcal{T}_i}^r)$, where $\mathbf{u} = \{\alpha\}$ and by (iii) setting the predictor’s meta-parameters to the empty set $\mathbf{w} = \emptyset$. Equation (5) applies with no modifications. **MT-net** (Lee and Choi 2018) is a variant of MAML in which the predictor’s meta-parameter set \mathbf{w} is not empty. The part of the predictor parameterized with \mathbf{w} is meta-learned

across tasks and is fixed during task adaptation.

Optimization as a model for few-shot learning (Ravi and Larochelle 2016) can be derived from (4) and (5) via the following steps (in addition to those of MAML). First, set the update function \mathcal{U}_u to the update equation of an LSTM-like cell of the form (ℓ is the LSTM update step index) $\theta_\ell \leftarrow f_\ell \theta_{\ell-1} + \alpha_\ell \nabla_{\theta_{\ell-1}} \mathcal{L}_{\mathcal{T}_i}(\mathcal{P}_{\theta_{\ell-1}, \mathbf{w}}(\mathcal{X}_{\mathcal{T}_i}^r), \mathcal{Y}_{\mathcal{T}_i}^r)$. Second, set f_ℓ to be the LSTM forget gate value (Ravi and Larochelle 2016): $f_\ell = \sigma(\mathbf{W}_F[\nabla_{\theta} \mathcal{L}_{\mathcal{T}_i}, \mathcal{L}_{\mathcal{T}_i}, \theta_{\ell-1}, f_{\ell-1}] + \mathbf{b}_F)$ and α_ℓ to be the LSTM input gate value: $\alpha_\ell = \sigma(\mathbf{W}_\alpha[\nabla_{\theta} \mathcal{L}_{\mathcal{T}_i}, \mathcal{L}_{\mathcal{T}_i}, \theta_{\ell-1}, \alpha_{\ell-1}] + \mathbf{b}_\alpha)$. Here σ is a sigmoid non-linearity. Finally, include all the LSTM parameters into the set of update meta-parameters: $\mathbf{u} = \{\mathbf{W}_F, \mathbf{b}_F, \mathbf{W}_\alpha, \mathbf{b}_\alpha\}$.

Prototypical Networks (PNs) (Snell, Swersky, and Zemel 2017). Most metric-based meta-learning approaches, including PNs, rely on comparing embeddings of the task training set with those of the validation set. Therefore, it is convenient to consider a composite predictor consisting of the *embedding* function, \mathcal{E}_w , and the *comparison* function, \mathcal{C}_θ , $\mathcal{P}_{\theta, \mathbf{w}}(\cdot) = \mathcal{C}_\theta \circ \mathcal{E}_w(\cdot)$. PNs can be derived from (4) and (5) by considering a K -shot image classification task, convolutional network \mathcal{E}_w shared across tasks and class prototypes $\mathbf{p}_k = \frac{1}{K} \sum_j y_j^r = k \mathcal{E}_w(\mathcal{X}_i^r)$ included in $\theta = \{\mathbf{p}_k\}_{\forall k}$. Initialization function $\mathcal{J}_{\mathbf{t}_0}$ with $\mathbf{t}_0 = \emptyset$ simply sets θ to the values of prototypes. \mathcal{U}_u is an identity map with $\mathbf{u} = \emptyset$ and \mathcal{C}_θ is as a softmax classifier:

$$y_{\mathcal{T}_i}^{val} = \arg \max_k \text{softmax}(-d(\mathcal{E}_w(\mathcal{X}_{\mathcal{T}_i}^{val}), \mathbf{p}_k)). \quad (6)$$

Here $d(\cdot, \cdot)$ is a similarity measure and the softmax is normalized w.r.t. all \mathbf{p}_k . Finally, define the loss $\mathcal{L}_{\mathcal{T}_i}$ in (5) as the cross-entropy of the softmax classifier described in (6). Interestingly, $\theta = \{\mathbf{p}_k\}_{\forall k}$ are nothing else than the dynamically generated weights of the final linear layer fed into the softmax, which is especially apparent when $d(\mathbf{a}, \mathbf{b}) = -\mathbf{a} \cdot \mathbf{b}$. The fact that in the prototypical network scenario only the final linear layer weights are dynamically generated based on the task training set resonates very well with the most recent study of MAML (Raghu et al. 2019). It has been shown that most of the MAML’s gain can be recovered by only adapting the weights of the final linear layer in the inner loop.

Matching networks (Vinyals et al. 2016) are similar to PNs with a few adjustments. In the *vanilla* matching network architecture, \mathcal{C}_θ is defined, assuming one-hot encoded $y_{\mathcal{T}_i}^{val}$ and $y_{\mathcal{T}_i}^r$, as a soft nearest neighbor:

$$\hat{y}_{\mathcal{T}_i}^{val} = \sum_{\mathbf{x}, \mathbf{y} \in \mathcal{D}_{\mathcal{T}_i}^r} \text{softmax}(-d(\mathcal{E}_w(\mathcal{X}_{\mathcal{T}_i}^{val}), \mathcal{E}_w(\mathbf{x}))) \mathbf{y}.$$

The softmax is normalized w.r.t. $\mathbf{x} \in \mathcal{D}_{\mathcal{T}_i}^r$. Predictor parameters, dynamically generated by $\mathcal{J}_{\mathbf{t}_0}$, include embedding/label pairs: $\theta = \{(\mathcal{E}_w(\mathbf{x}), \mathbf{y}), \forall \mathbf{x}, \mathbf{y} \in \mathcal{D}_{\mathcal{T}_i}^r\}$. In the *FCE* matching network, validation and training embeddings additionally interact with the task training set via attention LSTMs (Vinyals et al. 2016). To reflect this, the update function, $\mathcal{U}_u(\theta, \mathcal{D}_{\mathcal{T}_i}^r)$, updates the original embeddings via LSTM equations: $\theta \leftarrow \{(\text{attLSTM}_u[\mathcal{E}_w(\mathbf{x}), \mathcal{D}_{\mathcal{T}_i}^r], \mathbf{y}), \forall \mathbf{x}, \mathbf{y} \in \mathcal{D}_{\mathcal{T}_i}^r\}$. The LSTM parameters are included in \mathbf{u} . Second, the predictor is augmented with an additional relation module \mathcal{R}_{w_R} , such that

$\mathcal{P}_{\theta, \mathbf{w}}(\cdot) = \mathcal{C}_\theta \circ \mathcal{R}_{w_R} \circ \mathcal{E}_{w_E}(\cdot)$, with the set of predictor meta-parameters extended accordingly: $\mathbf{w} = (\mathbf{w}_R, \mathbf{w}_E)$. The relation module is again implemented via LSTM: $\mathcal{R}_{w_R}(\cdot) \equiv \text{attLSTM}_{w_R}(\cdot, \mathcal{D}_{\mathcal{T}_i}^r)$.

TADAM (Oreshkin, Rodríguez López, and Lacoste 2018) extends PNs by dynamically conditioning the embedding function on the task training data via FiLM layers (Perez et al. 2018). TADAM’s predictor has the following form: $\mathcal{P}_{\theta, \mathbf{w}}(\cdot) = \mathcal{C}_{\theta_c} \circ \mathcal{E}_{\theta_{\gamma, \beta}, \mathbf{w}}(\cdot)$; $\theta = (\theta_{\gamma, \beta}, \theta_c)$. The compare function parameters are as before, $\theta_c = \{\mathbf{p}_k\}_{\forall k}$. The embedding function parameters $\theta_{\gamma, \beta}$ include the FiLM layer γ/β (scale/shift) vectors for each convolutional layer, generated by a separate FC network from the task embedding. The initialization function $\mathcal{J}_{\mathbf{t}_0}$ sets $\theta_{\gamma, \beta}$ to all zeros, embeds task training data, and sets the task embedding to the average of class prototypes. The update function \mathcal{U}_u whose meta-parameters include the coefficients of the FC network, $\mathbf{u} = \mathbf{w}_{FC}$, generates an update to $\theta_{\gamma, \beta}$ from the task embedding. Then it generates an update to the class prototypes θ_c using $\mathcal{E}_{\theta_{\gamma, \beta}, \mathbf{w}}(\cdot)$ conditioned with the updated $\theta_{\gamma, \beta}$.

LEO (Rusu et al. 2019) uses a fixed pretrained embedding function. The intermediate low-dimensional latent space \mathbf{z} is optimized and is used to generate the predictor’s task-adaptive final layer weights θ_c . LEO’s predictor, $\mathcal{P}_{\theta, \mathbf{w}}(\cdot) = \mathcal{C}_\theta \circ \mathcal{E}(\cdot)$ has final layer and the latent space parameters, $\theta = (\theta_c, \theta_z)$, and no meta-parameters, $\mathbf{w} = \emptyset$. The initialization function $\mathcal{J}_{\mathbf{t}_0}$, $\mathbf{t}_0 = (\mathbf{w}_E, \mathbf{w}_R)$, uses a task encoder and a relation network with meta-parameters \mathbf{w}_E and \mathbf{w}_R . It meta-initializes the latent space parameters, θ_z , based on the task training data. The update function \mathcal{U}_u , $\mathbf{u} = \mathbf{w}_D$, uses a decoder with meta-parameters \mathbf{w}_D to iteratively decode θ_z into the final layer weights, θ_c . It optimizes θ_z by executing gradient descent $\theta_z \leftarrow \theta_z - \alpha \nabla_{\theta_z} \mathcal{L}_{\mathcal{T}_i}(\mathcal{P}_\theta(\mathcal{X}_{\mathcal{T}_i}^r), \mathcal{Y}_{\mathcal{T}_i}^r)$ in the inner loop.

In this section, we illustrated that seven distinct meta-learning algorithms from two broad categories (optimization- and metric-based) can be derived from our equations (4) and (5). This confirms that our meta-learning framework is general and it can represent existing meta-learning algorithms.

3 N-BEATS as a Meta-learning Algorithm

Let us now focus on the analysis of N-BEATS described by equations (2), (3). We first introduce the following notation: $f : \mathbf{x}_\ell \mapsto \mathbf{h}_{\ell, 4}$; $g : \mathbf{h}_{\ell, 4} \mapsto \hat{\mathbf{y}}_\ell$; $q : \mathbf{h}_{\ell, 4} \mapsto \hat{\mathbf{x}}_\ell$. In the original equations, g and q are linear and hence can be represented by equivalent matrices \mathbf{G} and \mathbf{Q} . In the following, we keep the notation general as much as possible, transitioning to the linear case only when needed. Then, given the network input, \mathbf{x} ($\mathbf{x}_1 \equiv \mathbf{x}$), and noting that $\hat{\mathbf{x}}_{\ell-1} = q \circ f(\mathbf{x}_{\ell-1})$ we can write N-BEATS as follows:

$$\hat{\mathbf{y}} = g \circ f(\mathbf{x}) + \sum_{\ell > 1} g \circ f(\mathbf{x}_{\ell-1} - q \circ f(\mathbf{x}_{\ell-1})). \quad (7)$$

N-BEATS is now derived from the meta-learning framework of Sec. 2 using two observations: (i) each application of $g \circ f$ in (7) is a predictor and (ii) each block of N-BEATS is the iteration of the inner meta-learning loop. More concretely, we have that $\mathcal{P}_{\theta, \mathbf{w}}(\cdot) = g_{w_g} \circ f_{w_f, \theta}(\cdot)$. Here w_g and w_f are parameters of functions g and f , included in $\mathbf{w} = (w_g, w_f)$

and learned across tasks in the outer loop. The task-specific parameters θ consist of the sequence of input shift vectors, $\theta \equiv \{\mu_\ell\}_{\ell=0}^L$, defined such that the ℓ -th block input can be written as $\mathbf{x}_\ell = \mathbf{x} - \mu_{\ell-1}$. This yields a recursive expression for the predictor’s task-specific parameters of the form $\mu_\ell \leftarrow \mu_{\ell-1} + \widehat{\mathbf{x}}_\ell$, $\mu_0 \equiv \mathbf{0}$, obtained by recursively unrolling eq. (3). These yield the following initialization and update functions: $\mathcal{J}_{\mathbf{t}_0}$ with $\mathbf{t}_0 = \emptyset$ sets μ_0 to zero; $\mathcal{U}_{\mathbf{u}}$, with $\mathbf{u} = (\mathbf{w}_q, \mathbf{w}_f)$ generates a next parameter update based on $\widehat{\mathbf{x}}_\ell$:

$$\mu_\ell \leftarrow \mathcal{U}_{\mathbf{u}}(\mu_{\ell-1}, \mathcal{D}_{\mathcal{J}_i}^{\prime\prime}) \equiv \mu_{\ell-1} + q_{\mathbf{w}_q} \circ f_{\mathbf{w}_f}(\mathbf{x} - \mu_{\ell-1}).$$

Interestingly, (i) meta-parameters \mathbf{w}_f are shared between the predictor and the update function and (ii) the task training set is limited to the network input, $\mathcal{D}_{\mathcal{J}_i}^{\prime\prime} \equiv \{\mathbf{x}\}$. Note that the latter makes sense because the data are complete time series, with the inputs \mathbf{x} having the same form of internal dependencies as the forecasting targets \mathbf{y} . Hence, observing \mathbf{x} is enough to infer how to predict \mathbf{y} from \mathbf{x} in a way that is similar to how different parts of \mathbf{x} are related to each other.

Finally, according to (7), predictor outputs corresponding to the values of parameters θ learned at every iteration of the inner loop are combined in the final output. This corresponds to choosing a predictor of the form $\mathcal{P}_{\mu_{0:L}, \mathbf{w}}(\cdot) = \sum_{j=0}^L \omega_j \mathcal{P}_{\mu_j, \mathbf{w}}(\cdot)$, $\omega_j = 1, \forall j$ in (5). The outer learning loop (5) describes the N-BEATS training procedure across tasks (TS) with no modification.

Remark 3.1. It is clear that the final output of the architecture depends on the sequence $\mu_{0:L}$. Quite obviously, even if predictor parameters $\mathbf{w}_g, \mathbf{w}_f$ are shared across blocks and fixed, the behaviour of $\mathcal{P}_{\mu_{0:L}, \mathbf{w}}(\cdot) = g_{\mathbf{w}_g} \circ f_{\mathbf{w}_f, \mu_{0:L}}(\cdot)$ is governed by an extended space of parameters $(\mathbf{w}, \mu_1, \mu_2, \dots)$. Therefore, the expressive power of the architecture can be expected to grow with the growing number of blocks, in proportion to the growth of the space spanned by $\mu_{0:L}$, even if $\mathbf{w}_g, \mathbf{w}_f$ are shared across blocks. It is reasonable to expect that the addition of identical blocks will improve generalization performance, because of the increase in expressive power, as each block extracts more information from \mathbf{x} and expands the set of predictor parameters via meta-learning inner loop iteration.

3.1 Linear Approximation Analysis

Next, we go a level deeper in the analysis to uncover more intricate task adaptation processes. Using linear approximation analysis, we express N-BEATS’ meta-learning operation in terms of the adaptation of the internal weights of the network based on the task input data. In particular, assuming small $\widehat{\mathbf{x}}_\ell$, (7) can be approximated using the first order Taylor series expansion in the vicinity of $\mathbf{x}_{\ell-1}$:

$$\widehat{\mathbf{y}} = g \circ f(\mathbf{x}) + \sum_{\ell > 1} [g - \mathbf{J}_{g \circ f}(\mathbf{x}_{\ell-1})q] \circ f(\mathbf{x}_{\ell-1}) + o(\|q \circ f(\mathbf{x}_{\ell-1})\|).$$

Here $\mathbf{J}_{g \circ f}(\mathbf{x}_{\ell-1}) = \mathbf{J}_g(f(\mathbf{x}_{\ell-1}))\mathbf{J}_f(\mathbf{x}_{\ell-1})$ is the Jacobian of $g \circ f$. We now consider linear g and q , as mentioned earlier, in which case g and q are represented by two matrices of appropriate dimensionality, \mathbf{G} and \mathbf{Q} ; and $\mathbf{J}_g(f(\mathbf{x}_{\ell-1})) = \mathbf{G}$. Thus, the above expression can be simplified as:

$$\widehat{\mathbf{y}} = \mathbf{G}f(\mathbf{x}) + \sum_{\ell > 1} \mathbf{G}[\mathbf{I} - \mathbf{J}_f(\mathbf{x}_{\ell-1})\mathbf{Q}]f(\mathbf{x}_{\ell-1}) + o(\|\mathbf{Q}f(\mathbf{x}_{\ell-1})\|).$$

Continuously applying the linear approximation $f(\mathbf{x}_\ell) = [\mathbf{I} - \mathbf{J}_f(\mathbf{x}_{\ell-1})\mathbf{Q}]f(\mathbf{x}_{\ell-1}) + o(\|\mathbf{Q}f(\mathbf{x}_{\ell-1})\|)$ until we reach $\ell = 1$ and recalling that $\mathbf{x}_1 \equiv \mathbf{x}$ we arrive at the following:

$$\widehat{\mathbf{y}} = \sum_{\ell > 0} \mathbf{G} \left[\prod_{k=1}^{\ell-1} [\mathbf{I} - \mathbf{J}_f(\mathbf{x}_{\ell-k})\mathbf{Q}] \right] f(\mathbf{x}) + o(\|\mathbf{Q}f(\mathbf{x}_\ell)\|). \quad (8)$$

Note that $\mathbf{G} \left(\prod_{k=1}^{\ell-1} [\mathbf{I} - \mathbf{J}_f(\mathbf{x}_{\ell-k})\mathbf{Q}] \right)$ can be written in the iterative update form. Consider $\mathbf{G}'_1 = \mathbf{G}$, then the update equation for \mathbf{G}' can be written as $\mathbf{G}'_\ell = \mathbf{G}'_{\ell-1}[\mathbf{I} - \mathbf{J}_f(\mathbf{x}_{\ell-1})\mathbf{Q}]$, $\forall \ell > 1$ and (8) becomes:

$$\widehat{\mathbf{y}} = \sum_{\ell > 0} \mathbf{G}'_\ell f(\mathbf{x}) + o(\|\mathbf{Q}f(\mathbf{x}_\ell)\|). \quad (9)$$

Let us now discuss how (9) can be used to re-interpret N-BEATS as an instance of the meta-learning framework (4) and (5). The predictor can now be represented in a decoupled form $\mathcal{P}_{\theta, \mathbf{w}}(\cdot) = g_\theta \circ f_{\mathbf{w}_f}(\cdot)$. Thus task adaptation is clearly confined in the decision function, g_θ , whereas the embedding function $f_{\mathbf{w}_f}$ only relies on fixed meta-parameters \mathbf{w}_f . The adaptive parameters θ include the sequence of projection matrices $\{\mathbf{G}'_\ell\}$. The meta-initialization function $\mathcal{J}_{\mathbf{t}_0}$ is parameterized with $\mathbf{t}_0 \equiv \mathbf{G}$ and it simply sets $\mathbf{G}'_1 \leftarrow \mathbf{t}_0$. The main ingredient of the update function $\mathcal{U}_{\mathbf{u}}$ is $\mathbf{Q}f_{\mathbf{w}_f}(\cdot)$, parameterized as before with $\mathbf{u} = (\mathbf{Q}, \mathbf{w}_f)$. The update function now consists of two equations:

$$\begin{aligned} \mathbf{G}'_\ell &\leftarrow \mathbf{G}'_{\ell-1}[\mathbf{I} - \mathbf{J}_f(\mathbf{x} - \mu_{\ell-1})\mathbf{Q}], \quad \forall \ell > 1, \\ \mu_\ell &\leftarrow \mu_{\ell-1} + \mathbf{Q}f_{\mathbf{w}_f}(\mathbf{x} - \mu_{\ell-1}), \quad \mu_0 = \mathbf{0}. \end{aligned} \quad (10)$$

Remark 3.2. The first order analysis results (9) and (10) suggest that under certain circumstances, the block-by-block manipulation of the input sequence apparent in (7) is equivalent to producing an iterative update of predictor’s final linear layer weights apparent in (10), with the block input being set to the same fixed value. This is very similar to the final linear layer update behaviour identified in other meta-learning algorithms: in LEO it is present by design (Rusu et al. 2019), in MAML it was identified by Raghu et al. (2019), and in PNs it follows from the results of our analysis in Section 2.2.

In this section we established that N-BEATS is an instance of a meta-learning algorithm described by equations (4) and (5). We showed that each block of N-BEATS is an inner meta-learning loop that generates additional shift parameters specific to the input time series. Therefore, the expressive power of the architecture is expected to grow with each additional block, even if all blocks share their parameters. We used linear approximation analysis to show that the input shift in a block is equivalent to the update of the block’s final linear layer weights under certain conditions. The key role in this process seems to be encapsulated in the non-linearity of f and in \mathbf{Q} generating the sequence of input shifts μ_ℓ and rejections of \mathbf{J}_f . We study these aspects in more detail in Appendices D.1 and D.2.

4 Empirical Results

We evaluate performance on a number of datasets representing a diverse set of univariate time series. For each of

Table 1: Dataset-specific metrics aggregated over each dataset; lower values are better. The bottom three rows represent the zero-shot transfer setup, indicating respectively the core algorithm (DeepAR or N-BEATS) and the source dataset (M4 or FR(ED)). All other model names are explained in Appendix F. †N-BEATS trained on double upsampled monthly data, see Appendix C. ‡M3/M4 SMAPE definitions differ. *DeepAR trained by us using GluonTS.

M4, SMAPE		M3, SMAPE [‡]		TOURISM, MAPE		ELECTR / TRAFF, ND		FRED, SMAPE	
Pure ML	12.89	Comb	13.52	ETS	20.88	MatFact	0.16 / 0.20	ETS	14.16
Best STAT	11.99	ForePro	13.19	Theta	20.88	DeepAR	0.07 / 0.17	Naïve	12.79
ProLogistica	11.85	Theta	13.01	ForePro	19.84	DeepState	0.08 / 0.17	SES	12.70
Best ML/TS	11.72	DOTM	12.90	Strato	19.52	Theta	0.08 / 0.18	Theta	12.20
DL/TS hybrid	11.37	EXP	12.71	LCBaker	19.35	ARIMA	0.07 / 0.15	ARIMA	12.15
N-BEATS	11.14		12.37		18.52		0.07 / 0.11		11.49
DeepAR*	12.25		12.67		19.27		0.09 / 0.19		n/a
DeepAR-M4*	n/a		14.76		24.79		0.15 / 0.36		n/a
N-BEATS-M4	n/a		12.44		18.82		0.09 / 0.15		11.60
N-BEATS-FR	11.70		12.69		19.94	†	0.09 / 0.26		n/a

them, we evaluate the base N-BEATS performance compared against the best-published approaches (to the authors’ knowledge). We also evaluate zero-shot transfer from several source datasets, as explained next.

Base datasets. **M4** (M4 Team 2018), contains 100k TS representing demographic, finance, industry, macro and micro indicators. Sampling frequencies include yearly, quarterly, monthly, weekly, daily and hourly. **M3** (Makridakis and Hibon 2000) contains 3003 TS from domains and sampling frequencies similar to M4. **FRED** is a dataset introduced in this paper containing 290k US and international economic TS from 89 sources, a subset of the data published by the Federal Reserve Bank of St. Louis (Federal Reserve 2019). **TOURISM** (Athanasopoulos et al. 2011) includes monthly, quarterly and yearly series of indicators related to tourism activities. **ELECTRICITY** (Dua and Graff 2017; Yu, Rao, and Dhillon 2016) represents the hourly electricity usage of 370 customers. **TRAFFIC** (Dua and Graff 2017; Yu, Rao, and Dhillon 2016) tracks hourly occupancy rates of 963 lanes in the Bay Area freeways. Additional details for all datasets appear in Appendix E.

Zero-shot time-series forecasting task definition. One of the base datasets, a *source* dataset, is used to train a machine learning model. The trained model then forecasts a TS in a *target* dataset. The source and the target datasets are distinct: they do not contain TS whose values are linear transformations of each other. The forecasted TS is split into two non-overlapping pieces: the history, and the test. The history is used as model input and the test is used to compute the forecast error metric. We use the history and the test splits for the base datasets consistent with their original publication, unless explicitly stated otherwise. To produce forecasts, the model is allowed to access the TS in the target dataset on a *one-at-a-time* basis. This is to avoid having the model implicitly learn/adapt based on any information contained in the target dataset other than the history of the forecasted TS. If any adjustments of model parameters or hyperparameters are necessary, they are allowed *exclusively* using the history

of the forecasted TS.

Training setup. DeepAR (Salinas et al. 2019) is trained using GluonTS implementation from its authors (Alexandrov et al. 2019). N-BEATS is trained following the original training setup of Oreshkin et al. (2020). Both N-BEATS and DeepAR are trained with scaling/descaling the architecture input/output by dividing/multiplying all input/output values by the max value of the input window. This does not affect the accuracy of the models in the usual train/test scenario. In the zero-shot regime, this operation is intended to prevent catastrophic failure when the scale of the target dataset differs significantly from that of the source dataset. Additional training setup details are provided in Appendix C.

Key results. For each dataset, we compare our results to 5 representative entries reported in the literature for that dataset, based on dataset-specific metrics (M4, FRED, M3: SMAPE; TOURISM: MAPE; ELECTRICITY, TRAFFIC: ND). We additionally train the popular machine learning TS model DeepAR and evaluate it in the zero-shot regime. Our main results appear in Table 1, with more details provided in Appendix F. In the zero-shot forecasting regime (bottom three rows), N-BEATS consistently outperforms most statistical models tailored to these datasets as well as DeepAR trained on M4 and evaluated in zero-shot regime on other datasets. N-BEATS trained on FRED and applied in the zero-shot regime to M4 outperforms the best statistical model selected for its performance on M4 and is at par with the competition’s second entry (boosted trees). On M3 and TOURISM the zero-shot forecasting performance of N-BEATS is better than that of the M3 winner, Theta (Assimakopoulos and Nikolopoulos 2000). On ELECTRICITY and TRAFFIC N-BEATS performs close to or better than other neural models trained on these datasets. The results suggest that a neural model is able to extract general knowledge about TS forecasting and then successfully adapt it to forecast on unseen TS. Our study presents the first successful application of a neural model to solve univariate zero-shot TS point forecasting across a large variety of datasets, and suggest that a pre-trained N-BEATS

model can constitute a strong baseline for this task.

Meta-learning Effects. Remark 3.1 implies that N-BEATS internally generates a sequence of parameters that dynamically extend the expressive power of the architecture with each newly added block, even if the blocks are identical. To validate this hypothesis, we performed an experiment studying the zero-shot forecasting performance of N-BEATS with increasing number of blocks, with and without parameter sharing. The architecture was trained on M4 and the performance was measured on the target datasets M3 and TOURISM. The results are presented in Fig. 1. On the two datasets and for the shared-weights configuration, we consistently see performance improvement when the number of blocks increases up to about 30 blocks. In the same scenario, increasing the number of blocks beyond 30 leads to small, but consistent deterioration in performance. One can view these results as evidence supporting the meta-learning interpretation of N-BEATS, with a possible explanation of this phenomenon as overfitting in the meta-learning inner loop. It would not otherwise be obvious how to explain the generalization dynamics in Fig. 1. Additionally, the performance improvement due to meta-learning alone (shared weights, multiple blocks vs. a single block) is 12.60 to 12.44 (1.2%) and 20.40 to 18.82 (7.8%) for M3 and TOURISM, respectively (see Fig. 1). The performance improvement due to meta-learning and unique weights¹ (unique weights, multiple blocks vs. a single block) is 12.60 to 12.40 (1.6%) and 20.40 to 18.91 (7.4%). Clearly, the majority of the gain is due to the meta-learning alone. The introduction of unique block weights sometimes results in marginal gain, but often leads to a loss (see more results in Appendix G).

In this section, we presented empirical evidence that neural networks are able to provide high-quality zero-shot forecasts on unseen TS. We further empirically supported the hypothesis that meta-learning adaptation mechanisms identified within N-BEATS in Section 3 are instrumental in achieving impressive zero-shot forecasting accuracy results.

5 Discussion and Conclusion

Zero-shot transfer learning. We propose a broad meta-learning framework and explain mechanisms facilitating zero-shot forecasting. Our results show that neural networks can extract generic knowledge about forecasting and apply it in zero-shot transfer, with N-BEATS providing a strong baseline for univariate time series forecasting across several datasets. **Residual architectures** in general are covered by the analysis of Sec. 3, which might explain some of the success of residual architectures, although their deeper study should be subject to future work. **Algorithm design implications.** Our theory suggests that residual connections produce, on-the-fly, compact task-specific parameter updates for identical blocks. This mechanism makes sharing weights across residual blocks effective, resulting in networks with reduced memory footprint and comparable statistical performance.

¹Intuitively, the network with unique block weights includes the network with identical weights as a special case. Therefore, it is free to combine the effect of meta-learning with the effect of unique block weights based on its training loss.

We further empirically show that the generalization performance indeed increases if identical blocks are stacked and Sec. 3.1 reinterprets our results showing that, as a first-order approximation, N-BEATS produces an iterative update to the predictor final linear layer, uncovering a number of promising directions for architectural exploration. For example, it suggests that some of the well-established gradient-based meta-learning algorithms, such as MAML, could be effective in the context of TS forecasting when applied to simple fully-connected architectures such as a single N-BEATS block, or even the final layer thereof. There is also a clear parallel between our eq. (10) and the LSTM-based optimization approach (Ravi and Larochelle 2016). Finally, taking into account that N-BEATS performs a sequential update of the final linear layer and sums contributions of individual blocks, and making parallels with the stochastic optimization literature, we hypothesize that further improvements could be achieved by applying proper annealing of parameter updates across blocks, turning (9) into a form of Polyak averaging. **Memory efficiency and knowledge compression.** Our empirical results imply that N-BEATS is able to compress all the relevant knowledge about a given dataset in a single block, rather than in 10 or 30 blocks with individual weights. From a practical perspective, this could be used to obtain 10–30 times neural network weight compression and is relevant in applications where storing neural networks efficiently is important.

Broader Impacts and Ethical Considerations

Time series forecasting is central to the actions of intelligent agents: the ability to plan and control as well as to appropriately react to manifestations of complex partially or completely unknown systems often relies on the ability to forecast relevant observations based on their past history. Moreover, for most utility-maximizing agents, any gain in forecasting accuracy broadly translates into a utility gain; as such, improvements in forecasting technology can have wide impacts. The applications of forecasting span a variety of fields, ranging from high-frequency control (e.g. vehicle and robot control (Tang and Salakhutdinov 2019), data center optimization (Gao 2014)), to business planning (supply chain management (Leung 1995), workforce management (Chapados et al. 2014), forecasting phone call arrivals (Ibrahim et al. 2016) and customer traffic (Lam, Vandenbosch, and Pearce 1998)) and finally to ones that may be critical for the future survival of humanity, such as precision agriculture (Rodrigues Jr et al. 2019) or fire and flood management (Mahoo et al. 2015; Sit and Demir 2019). In business specifically, each percent point gain in accuracy can translate into millions of dollars in savings, for instance through better production planning (leading to less waste) and less transportation (reducing CO₂ emissions) (Kahn 2003; Kerkkänen, Korpela, and Huiskonen 2009; Nguyen, Ni, and Rossetti 2010).

The methods studied in this paper apply generally to univariate time series measured in discrete time, and do not focus on any one application area. As such, we can expect their practical impact to be quite broad. Nonetheless, significant limitations must also be noted: **(i) Non-stationarities:** the model, as presented, assumes that the future, broadly, can be predicted from the past. It does not contain explicit mecha-

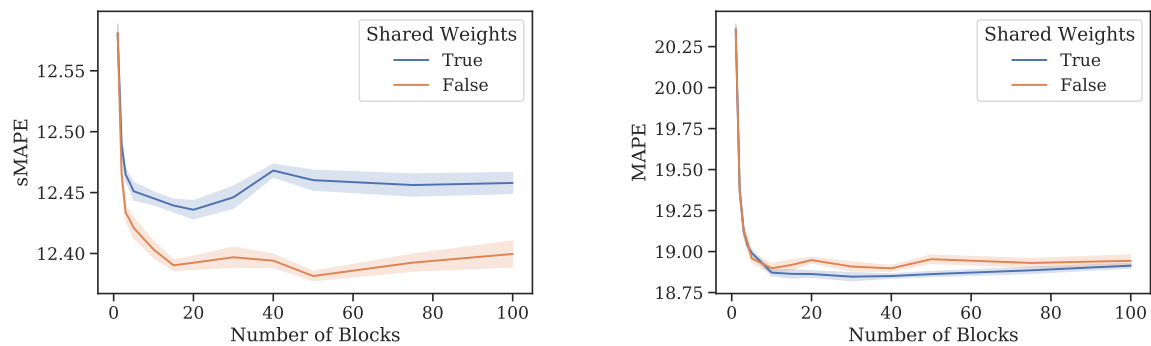


Figure 1: Zero-shot forecasting performance of N-BEATS trained on M4 and applied to M3 (**left**) and TOURISM (**right**) target datasets with respect to the number of blocks, L . The mean and one standard deviation interval (based on ensemble bootstrap) with (blue) and without (red) weight sharing across blocks are shown. The extended set of results for all datasets, using FRED as a source dataset and a few metrics are provided in Appendix G, further reinforcing our findings.

nisms to detect important structural breaks in the data that might invalidate what could be learned from past observations. **(ii) Transfer might not work:** even though the results presented in this paper experiment with source datasets exhibiting a large diversity of time series for the purposes of transfer learning, one should exercise care before applying zero-shot transfer models to datasets with notably different characteristics. **(iii) Univariate point forecasts:** the methods introduced in this paper do not consider covariates nor distributional forecasting, yet those are important for a number of downstream applications (e.g. inventory planning). These can best be viewed as topics for future investigations. Moreover, even though the datasets studied in this paper span a broad range of practical applications, no benchmark study can possibly cover all imaginable use cases.

A risk arising from the above limitations centers around structural breaks and other non-stationarities: a non-expert user might come to place too much trust in a model whose deployment context has materially diverged from its training data. (One can witness the COVID-19 pandemic disruptions still underway at the time of writing to envision that historical data will hold limited utility in many economic and business forecasting tasks for the coming years.) As such, adequate care in user training should accompany model deployment, preferably equipping them (both users and models) with mechanisms to detect structural breaks.

References

Alexandrov, A.; Benidis, K.; Bohlke-Schneider, M.; Flunkert, V.; Gasthaus, J.; Januschowski, T.; Maddix, D. C.; Rangapuram, S.; Salinas, D.; Schulz, J.; Stella, L.; Türkmen, A. C.; and Wang, Y. 2019. GluonTS: Probabilistic Time Series Modeling in Python. *arXiv preprint arXiv:1906.05264*.

Assimakopoulos, V.; and Nikolopoulos, K. 2000. The theta model: a decomposition approach to forecasting. *International Journal of Forecasting* 16(4): 521–530.

Athanasopoulos, G.; and Hyndman, R. J. 2011. The value of feedback in forecasting competitions. *International Journal of Forecasting* 27(3): 845–849.

Athanasopoulos, G.; Hyndman, R. J.; Song, H.; and Wu, D. C.

2011. The tourism forecasting competition. *International Journal of Forecasting* 27(3): 822–844.

Baker, L. C.; and Howard, J. 2011. Winning methods for forecasting tourism time series. *International Journal of Forecasting* 27(3): 850–852.

Bengio, S.; Bengio, Y.; Cloutier, J.; and Gecsei, J. 1992. On the optimization of a synaptic learning rule. In *Optimality in Artificial and Biological Neural Networks*.

Bengio, Y.; Bengio, S.; and Cloutier, J. 1991. Learning a Synaptic Learning Rule. In *Proceedings of the International Joint Conference on Neural Networks, II–A969*. Seattle, USA.

Bergmeir, C.; Hyndman, R. J.; and Benítez, J. M. 2016. Bagging exponential smoothing methods using STL decomposition and Box–Cox transformation. *International Journal of Forecasting* 32(2): 303–312.

Chapados, N.; Joliveau, M.; L’Écuyer, P.; and Rousseau, L.-M. 2014. Retail store scheduling for profit. *European Journal of Operational Research* 239(3): 609 – 624.

Dua, D.; and Graff, C. 2017. UCI Machine Learning Repository. URL <http://archive.ics.uci.edu/ml>.

Engle, R. F. 1982. Autoregressive conditional heteroscedasticity with estimates of the variance of United Kingdom inflation. *Econometrica* 50(4): 987–1007.

Fawaz, H. I.; Forestier, G.; Weber, J.; Idoumghar, L.; and Muller, P.-A. 2018. Transfer learning for time series classification. *2018 IEEE International Conference on Big Data (Big Data)*.

Federal Reserve Bank of St. Louis. 2019. FRED Economic Data. Data retrieved from <https://fred.stlouisfed.org/> Accessed: 2019-11-01.

Finn, C.; Abbeel, P.; and Levine, S. 2017. Model-Agnostic Meta-Learning for Fast Adaptation of Deep Networks. In *ICML*, 1126–1135.

Fiorucci, J. A.; Pellegrini, T. R.; Louzada, F.; Petropoulos, F.; and Koehler, A. B. 2016. Models for optimising the theta method and their relationship to state space models. *International Journal of Forecasting* 32(4): 1151–1161.

Flunkert, V.; Salinas, D.; and Gasthaus, J. 2017. DeepAR: Probabilistic Forecasting with Autoregressive Recurrent Networks. *CoRR* abs/1704.04110.

- Gao, J. 2014. Machine learning applications for data center optimization. Technical report, Google.
- Gauss, C. F. 1809. *Theoria motus corporum coelestium in sectionibus conicis solem ambientium*. Hamburg: Frid. Perthes and I. H. Besser.
- Glorot, X.; Bordes, A.; and Bengio, Y. 2011. Deep Sparse Rectifier Neural Networks. In *AISTATS'2011*.
- Harlow, H. F. 1949. The Formation of Learning Sets. *Psychological Review* 56(1): 51–65. doi:10.1037/h0062474.
- Holt, C. C. 1957. Forecasting trends and seasonals by exponentially weighted averages. Technical Report ONR memorandum no. 5, Carnegie Institute of Technology, Pittsburgh, PA.
- Holt, C. C. 2004. Forecasting seasonals and trends by exponentially weighted moving averages. *International Journal of Forecasting* 20(1): 5–10.
- Hooshmand, A.; and Sharma, R. 2019. Energy Predictive Models with Limited Data Using Transfer Learning. In *Proceedings of the Tenth ACM International Conference on Future Energy Systems, e-Energy'19*, 12–16.
- Hyndman, R.; and Koehler, A. B. 2006. Another look at measures of forecast accuracy. *International Journal of Forecasting* 22(4): 679–688.
- Hyndman, R. J.; and Khandakar, Y. 2008. Automatic time series forecasting: the forecast package for R. *Journal of Statistical Software* 26(3): 1–22.
- Ibrahim, R.; Ye, H.; L'Ecuyer, P.; and Shen, H. 2016. Modeling and forecasting call center arrivals: A literature survey and a case study. *International Journal of Forecasting* 32(3): 865–874.
- Kahn, K. B. 2003. How to Measure the Impact of a Forecast Error on an Enterprise? *The Journal of Business Forecasting Methods & Systems* 22(1).
- Kerkkänen, A.; Korpela, J.; and Huiskonen, J. 2009. Demand forecasting errors in industrial context: Measurement and impacts. *International Journal of Production Economics* 118(1): 43–48.
- Lake, B. M.; Ullman, T. D.; Tenenbaum, J. B.; and Gershman, S. J. 2017. Building machines that learn and think like people. *Behavioral and Brain Sciences* 40: e253.
- Lam, S.; Vandenbosch, M.; and Pearce, M. 1998. Retail sales force scheduling based on store traffic forecasting. *Journal of Retailing* 74(1): 61–88.
- Lee, Y.; and Choi, S. 2018. Gradient-based meta-learning with learned layerwise metric and subspace. In *ICML*, 2933–2942.
- Leung, H. C. 1995. Neural networks in supply chain management. In *Proceedings for Operating Research and the Management Sciences*, 347–352.
- Li, Z.; Zhou, F.; Chen, F.; and Li, H. 2017. Meta-SGD: Learning to Learn Quickly for Few Shot Learning. *CoRR* abs/1707.09835.
- M4 Team. 2018. M4 competitor's guide: prizes and rules. URL www.m4.unic.ac.cy/wp-content/uploads/2018/03/M4-CompetitorsGuide.pdf.
- Mahoo, H.; Mbungu, W.; Yonah, I.; Recha, J.; Radeny, M.; Kimeli, P.; and Kinyangi, J. 2015. Integrating Indigenous Knowledge with Scientific Seasonal Forecasts for Climate Risk Management in Lushoto District in Tanzania. Technical Report CCAFS Working Paper No. 103, CGIAR research program on climate change, agriculture and food security.
- Makridakis, S.; Andersen, A.; Carbone, R.; Fildes, R.; Hibon, M.; Lewandowski, R.; Newton, J.; Parzen, E.; and Winkler, R. 1982. The accuracy of extrapolation (time series) methods: Results of a forecasting competition. *Journal of forecasting* 1(2): 111–153.
- Makridakis, S.; Chatfield, C.; Hibon, M.; Lawrence, M.; Mills, T.; Ord, K.; and Simmons, L. F. 1993. The M2-competition: A real-time judgmentally based forecasting study. *International Journal of Forecasting* 9(1): 5–22.
- Makridakis, S.; and Hibon, M. 2000. The M3-Competition: results, conclusions and implications. *International Journal of Forecasting* 16(4): 451–476.
- Makridakis, S.; Spiliotis, E.; and Assimakopoulos, V. 2018a. The M4-Competition: Results, findings, conclusion and way forward. *International Journal of Forecasting* 34(4): 802–808.
- Makridakis, S.; Spiliotis, E.; and Assimakopoulos, V. 2018b. Statistical and Machine Learning forecasting methods: Concerns and ways forward. *PLoS ONE* 13(3).
- Montero-Manso, P.; Athanasopoulos, G.; Hyndman, R. J.; and Tala-gala, T. S. 2020. FFORMA: Feature-based forecast model averaging. *International Journal of Forecasting* 36(1): 86–92.
- Nair, V.; and Hinton, G. E. 2010. Rectified Linear Units Improve Restricted Boltzmann Machines. In *ICML*, 807–814.
- Neale, A. A. 1985. Weather Forecasting: Magic, Art, Science and Hypnosis. *Weather and Climate* 5(1): 2–5.
- Nguyen, H.-N.; Ni, Q.; and Rossetti, M. D. 2010. Exploring the cost of forecast error in inventory systems. In *Proceedings of the 2010 Industrial Engineering Research Conference*.
- Oreshkin, B. N.; Carpov, D.; Chapados, N.; and Bengio, Y. 2020. N-BEATS: Neural basis expansion analysis for interpretable time series forecasting. In *ICLR*.
- Oreshkin, B. N.; Rodríguez López, P.; and Lacoste, A. 2018. TADAM: Task dependent adaptive metric for improved few-shot learning. In *NeurIPS*, 721–731.
- Perez, E.; Strub, F.; De Vries, H.; Dumoulin, V.; and Courville, A. 2018. FILM: Visual reasoning with a general conditioning layer. In *AAAI*.
- Petersen, K. B.; and Pedersen, M. S. 2012. The Matrix Cookbook. Version 20121115.
- Raghu, A.; Raghu, M.; Bengio, S.; and Vinyals, O. 2019. Rapid Learning or Feature Reuse? Towards Understanding the Effectiveness of MAML.
- Rangapuram, S. S.; Seeger, M.; Gasthaus, J.; Stella, L.; Wang, Y.; and Januschowski, T. 2018. Deep State Space Models for Time Series Forecasting. In *NeurIPS*.
- Ravi, S.; and Larochelle, H. 2016. Optimization as a model for few-shot learning. In *ICLR*.
- Ribeiro, M.; Grolinger, K.; ElYamany, H. F.; Higashino, W. A.; and Capretz, M. A. 2018. Transfer learning with seasonal and trend adjustment for cross-building energy forecasting. *Energy and Buildings* 165: 352–363.
- Rodrigues Jr, F. A.; Jabloun, M.; Ortiz-Monasterio, J. I.; Crout, N. M. J.; Gurusamy, S.; and Green, S. 2019. Mexican Crop Observation, Management and Production Analysis Services System — COMPASS. In *Poster Proceedings of the 12th European Conference on Precision Agriculture*.
- Rusu, A. A.; Rao, D.; Sygnowski, J.; Vinyals, O.; Pascanu, R.; Osindero, S.; and Hadsell, R. 2019. Meta-Learning with Latent Embedding Optimization. In *ICLR*.

- Salinas, D.; Flunkert, V.; Gasthaus, J.; and Januschowski, T. 2019. DeepAR: Probabilistic forecasting with autoregressive recurrent networks. *International Journal of Forecasting* .
- Schmidhuber, J. 1987. *Evolutionary principles in self-referential learning*. Master's thesis, Institut f. Informatik, Tech. Univ. Munich.
- Sezer, O. B.; Gudelek, M. U.; and Ozbayoglu, A. M. 2019. Financial Time Series Forecasting with Deep Learning : A Systematic Literature Review: 2005-2019.
- Sit, M.; and Demir, I. 2019. Decentralized flood forecasting using deep neural networks. *arXiv preprint arXiv:1902.02308* .
- Smyl, S. 2020. A hybrid method of exponential smoothing and recurrent neural networks for time series forecasting. *International Journal of Forecasting* 36(1): 75 – 85.
- Smyl, S.; and Kuber, K. 2016. Data Preprocessing and Augmentation for Multiple Short Time Series Forecasting with Recurrent Neural Networks. In *36th International Symposium on Forecasting*.
- Snell, J.; Swersky, K.; and Zemel, R. S. 2017. Prototypical Networks for Few-shot Learning. In *NIPS*, 4080–4090.
- Spiliotis, E.; Assimakopoulos, V.; and Nikolopoulos, K. 2019. Forecasting with a hybrid method utilizing data smoothing, a variation of the Theta method and shrinkage of seasonal factors. *International Journal of Production Economics* 209: 92–102.
- Syntetos, A. A.; Boylan, J. E.; and Croston, J. D. 2005. On the categorization of demand patterns. *Journal of the Operational Research Society* 56(5): 495–503.
- Tang, C.; and Salakhutdinov, R. R. 2019. Multiple Futures Prediction. In *NeurIPS* 32, 15398–15408.
- Velkoski, A. 2016. Python Client for FRED API. URL <https://github.com/avelkoski/FRB>.
- Vinyals, O.; Blundell, C.; Lillicrap, T.; Kavukcuoglu, K.; and Wierstra, D. 2016. Matching Networks for One Shot Learning. In *NIPS*, 3630–3638.
- Walker, G. 1931. On Periodicity in Series of Related Terms. *Proc. R. Soc. Lond. A* 131: 518–532.
- Wang, Y.; Smola, A.; Maddix, D. C.; Gasthaus, J.; Foster, D.; and Januschowski, T. 2019. Deep Factors for Forecasting. In *ICML*.
- Winters, P. R. 1960. Forecasting Sales by Exponentially Weighted Moving Averages. *Management Science* 6(3): 324–342.
- Yu, H.-F.; Rao, N.; and Dhillon, I. S. 2016. Temporal Regularized Matrix Factorization for High-dimensional Time Series Prediction. In *NIPS*.
- Yule, G. U. 1927. On a Method of Investigating Periodicities in Disturbed Series, with Special Reference to Wolfer's Sunspot Numbers. *Phil. Trans. the R. Soc. Lond. A* 226: 267–298.

Supplementary Material for A Strong Meta-Learned Baseline for Zero-Shot Time Series Forecasting

A TS Forecasting Accuracy Metrics

The following metrics are standard scale-free metrics in the practice of point forecasting performance evaluation (Hyndman and Koehler 2006; Makridakis and Hibon 2000; Makridakis, Spiliotis, and Assimakopoulos 2018a; Athanasopoulos et al. 2011): MAPE (Mean Absolute Percentage Error), SMAPE (symmetric MAPE) and MASE (Mean Absolute Scaled Error). Whereas SMAPE scales the error by the average between the forecast and ground truth, the MASE scales by the average error of the naïve predictor that simply copies the observation measured m periods in the past, thereby accounting for seasonality. Here m is the periodicity of the data (e.g., 12 for monthly series). OWA (overall weighted average) is a M4-specific metric used to rank competition entries (M4 Team 2018), where SMAPE and MASE metrics are normalized such that a seasonally-adjusted naïve forecast obtains $OWA = 1.0$. Normalized Deviation, ND, being a less standard metric in the traditional TS forecasting literature, is nevertheless quite popular in the machine learning TS forecasting papers (Yu, Rao, and Dhillon 2016; Flunkert, Salinas, and Gasthaus 2017; Wang et al. 2019; Rangapuram et al. 2018).

$$\begin{aligned} \text{SMAPE} &= \frac{200}{H} \sum_{i=1}^H \frac{|y_{T+i} - \hat{y}_{T+i}|}{|y_{T+i}| + |\hat{y}_{T+i}|}, \\ \text{MAPE} &= \frac{100}{H} \sum_{i=1}^H \frac{|y_{T+i} - \hat{y}_{T+i}|}{|y_{T+i}|}, \\ \text{MASE} &= \frac{1}{H} \sum_{i=1}^H \frac{|y_{T+i} - \hat{y}_{T+i}|}{\frac{1}{T+H-m} \sum_{j=m+1}^{T+H} |y_j - y_{j-m}|}, \\ \text{OWA} &= \frac{1}{2} \left[\frac{\text{SMAPE}}{\text{SMAPE}_{\text{Naïve2}}} + \frac{\text{MASE}}{\text{MASE}_{\text{Naïve2}}} \right], \\ \text{ND} &= \frac{\sum_{i,ts} |y_{T+i,ts} - \hat{y}_{T+i,ts}|}{\sum_{i,ts} |y_{T+i,ts}|}. \end{aligned}$$

In these expressions, y_t refers to the observed time series (ground truth) and \hat{y}_t refers to a point forecast. In the last equation, $y_{T+i,ts}$ refers to a sample $T+i$ from TS with index ts and the sum $\sum_{i,ts}$ is running over all TS indices and TS samples.

B N-BEATS Details

B.1 Architecture Details

N-BEATS originally proposed by (Oreshkin et al. 2020) optionally has interpretable hierarchical structure consisting of multiple stacks. In this work, without loss of generality, we focus on a generic model for which output partitioning is irrelevant. This is depicted in Figure 2, modified from Figure 1 in Oreshkin et al. (2020) accordingly. The final forecast

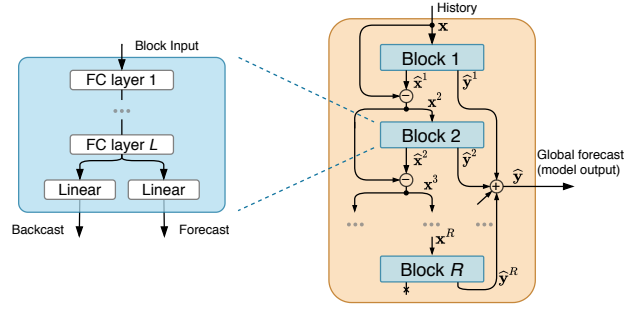


Figure 2: N-BEATS architecture, adapted from Figure 1 of Oreshkin et al. (2020).

is obtained from the sum of individual forecasts produced by blocks; the blocks are chained together using a doubly residual architecture.

C Training setup details

Most of the time, the model trained on a given frequency split of a source dataset is used to forecast the same frequency split on the target dataset. There are a few exceptions to this rule. First, when transferring from M4 to M3, the Others split of M3 is forecasted with the model trained on Quarterly split of M4. This is because (i) the default horizon length of M4 Quarterly is 8, same as that of M3 Others and (ii) M4 Others is heterogeneous and contains Weekly, Daily, Hourly data with horizon lengths 13, 14, 48. So M4 Quarterly to M3 Others transfer provided a more natural basis from an implementation standpoint. Second, the transfer from M4 to ELECTRICITY and TRAFFIC dataset is done based on a model trained on M4 Hourly. This is because ELECTRICITY and TRAFFIC contain hourly time-series with obvious 24-hour seasonality patterns. It is worth noting that the M4 Hourly only contains 414 time-series and we can clearly see positive zero-shot transfer in Table 1 from the model trained on this rather small dataset. Third, the transfer from FRED to ELECTRICITY and TRAFFIC is done by training the model on the FRED Monthly split, double upsampled using bi-linear interpolation. This is because FRED does not have hourly data. Monthly data naturally provide patterns with seasonality period 12. Upsampling with a factor of two and bi-linear interpolation provide data with natural seasonality period 24, most often observed in Hourly data, such as ELECTRICITY and TRAFFIC.

C.1 N-BEATS training setup

We use the same overall training framework, as defined by Oreshkin et al. (2020), including the stratified uniform sampling of TS in the source dataset to train the model. One model is trained per frequency split of a dataset (e.g. Yearly, Quarterly, Monthly, Weekly, Daily and Hourly frequencies in M4 dataset). All reported accuracy results are based on an ensemble of 30 models (5 different initializations with 6 different lookback periods). One aspect that we found important in the zero-shot regime, which is different from the original training setup, is the scaling/descaling of the input/output.

Table 2: DeepAR training parameters.

	Layers	Cells	Epochs	Batch Size
Yearly (M3, M4, Tourism)	3	40	300	32
Quarterly (M3, M4, Tourism)	2	20	100	32
Monthly (M3, M4, Tourism)	2	40	500	32
Others (M3)	2	40	100	32
M4 (weekly, daily)	3	20	100	32
M4 Hourly	2	20	50	32
Electricity (all splits)	2	40	50	64
Traffic (2008-01-14)	1	20	5	64
Traffic (other splits)	4	40	50	64

We scale/descale the architecture input/output by the dividing/multiplying all input/output values over the max value of the input window. We found that this does not affect the accuracy of the model trained and tested on the same dataset in a statistically significant way. In the zero-shot regime, this operation prevents catastrophic failure when the target dataset scale (marginal distribution) is significantly different from that of the source dataset.

C.2 DeepAR training setup

DeepAR experiments are using the model implementation provided by GluonTS (Alexandrov et al. 2019) version 1.6. We optimized hyperparameters of DeepAR as the defaults provided in GluonTS would often lead to apparently sub-optimal performance on many of the datasets. The training parameters for each dataset are described in Table 2. Weight decay is 0.0, Dropout rate is 0.0 for all experiments except Electricity dataset where it is 0.1. The default scaling was replaced by MaxAbs, which improved and stabilized results. All other parameters are defaults of *gluonts.model.deepar.DeepAREstimator*. To reduce variance of performance between experiments we use median ensemble of 30 independent runs. The code for DeepAR experiments can be found at https://github.com/timeseries-zeroshot/deepar_evaluation.

D Meta-learning Analysis Details

D.1 The Role of \mathbf{Q}

It is hard to study the form of \mathbf{Q} learned from the data in general. However, equipped with the results of the linear approximation analysis presented in Section 3.1, we can study the case of a two-block network, assuming that the L^2 norm loss between \mathbf{y} and $\hat{\mathbf{y}}$ is used to train the network. If, in addition, the dataset consists of the set of N pairs $\{\mathbf{x}^i, \mathbf{y}^i\}_{i=1}^N$ the dataset-wise loss \mathcal{L} has the following expression:

$$\mathcal{L} = \sum_i \|\mathbf{y}^i - 2\mathbf{G}f(\mathbf{x}^i) + \mathbf{J}_{gof}(\mathbf{x}^i)\mathbf{Q}f(\mathbf{x}^i) + o(\|\mathbf{Q}f(\mathbf{x}^i)\|)\|^2.$$

Introducing $\Delta\mathbf{y}^i = \mathbf{y}^i - 2\mathbf{G}f(\mathbf{x}^i)$, the error between the *default* forecast $2\mathbf{G}f(\mathbf{x}^i)$ and the ground truth \mathbf{y}^i , and expanding the

L^2 norm we obtain the following:

$$\begin{aligned} \mathcal{L} = & \sum_i \Delta\mathbf{y}^{i\top}\Delta\mathbf{y}^i + 2\Delta\mathbf{y}^{i\top}\mathbf{J}_{gof}(\mathbf{x}^i)\mathbf{Q}f(\mathbf{x}^i) \\ & + f(\mathbf{x}^i)^\top\mathbf{Q}^\top\mathbf{J}_{gof}^\top(\mathbf{x}^i)\mathbf{J}_{gof}(\mathbf{x}^i)\mathbf{Q}f(\mathbf{x}^i) + o(\|\mathbf{Q}f(\mathbf{x}^i)\|). \end{aligned}$$

Now, assuming that the rest of the parameters of the network are fixed, we have the derivative with respect to \mathbf{Q} using matrix calculus (Petersen and Pedersen 2012):

$$\begin{aligned} \frac{\partial\mathcal{L}}{\partial\mathbf{Q}} = & \sum_i 2\mathbf{J}_{gof}^\top(\mathbf{x}^i)\Delta\mathbf{y}^if(\mathbf{x}^i)^\top \\ & + 2\mathbf{J}_{gof}^\top(\mathbf{x}^i)\mathbf{J}_{gof}(\mathbf{x}^i)\mathbf{Q}f(\mathbf{x}^i)f(\mathbf{x}^i)^\top + o(\|\mathbf{Q}f(\mathbf{x}^i)\|). \end{aligned}$$

Using the above expression we conclude that the first-order approximation of optimal \mathbf{Q} satisfies the following equation:

$$\sum_i \mathbf{J}_{gof}^\top(\mathbf{x}^i)\Delta\mathbf{y}^if(\mathbf{x}^i)^\top = -\sum_i \mathbf{J}_{gof}^\top(\mathbf{x}^i)\mathbf{J}_{gof}(\mathbf{x}^i)\mathbf{Q}f(\mathbf{x}^i)f(\mathbf{x}^i)^\top.$$

Although this does not help to find a closed form solution for \mathbf{Q} , it does provide a quite obvious intuition: the LHS and the RHS are equal when $\Delta\mathbf{y}^i$ and $\mathbf{J}_{gof}(\mathbf{x}^i)\mathbf{Q}f(\mathbf{x}^i)$ are negatively correlated. Therefore, \mathbf{Q} satisfying the equation will tend to drive the update to \mathbf{G} in (10) in such a way that on average the projection of $f(\mathbf{x})$ over the update $\mathbf{J}_{gof}(\mathbf{x})\mathbf{Q}$ to matrix \mathbf{G} will tend to compensate the error $\Delta\mathbf{y}$ made by forecasting \mathbf{y} using \mathbf{G} based on meta-initialization.

D.2 Factors Enabling Meta-learning

Let us now analyze the factors that enable the meta-learning inner loop obvious in (10). First, and most straightforward, it is not viable without having multiple blocks connected via the backcast residual connection: $\mathbf{x}_\ell = \mathbf{x}_{\ell-1} - q \circ f(\mathbf{x}_{\ell-1})$. Second, the meta-learning inner loop is viable when f is non-linear: the update of \mathbf{G} is extracted from the curvature of f at the point dictated by the input \mathbf{x} and the sequence of shifts $\mu_{0:L}$. Indeed, suppose f is linear, and denote it by linear operator \mathbf{F} . The Jacobian $\mathbf{J}_f(\mathbf{x}_{\ell-1})$ becomes a constant, \mathbf{F} . Equation (8) simplifies as (note that for linear f , (8) is exact):

$$\hat{\mathbf{y}} = \sum_{\ell>0} \mathbf{G}[\mathbf{I} - \mathbf{F}\mathbf{Q}]^{\ell-1}\mathbf{F}\mathbf{x}.$$

Therefore, $\mathbf{G}\sum_{\ell>0}[\mathbf{I} - \mathbf{F}\mathbf{Q}]^{\ell-1}$ may be replaced with an equivalent \mathbf{G}' that is not data adaptive.

Remark D.1. Interestingly, $\sum_{\ell>0}[\mathbf{I} - \mathbf{F}\mathbf{Q}]^{\ell-1}$ happens to be a truncated Neumann series. Denoting Moore-Penrose pseudo-inverse as $[\cdot]^+$, assuming boundedness of $\mathbf{F}\mathbf{Q}$ and completing the series, $\sum_{\ell=0}^{\infty}[\mathbf{I} - \mathbf{F}\mathbf{Q}]^\ell$, results in $\hat{\mathbf{y}} = \mathbf{G}[\mathbf{F}\mathbf{Q}]^+\mathbf{F}\mathbf{x}$. Therefore, under certain conditions, the N-BEATS architecture with linear f and infinite number of blocks can be interpreted as a linear predictor of a signal in colored noise. Here the $[\mathbf{F}\mathbf{Q}]^+$ part cleans the intermediate space created by projection \mathbf{F} from the components that are undesired for forecasting and \mathbf{G} creates the forecast based on the initial projection $\mathbf{F}\mathbf{x}$ after it is “sanitized” by $[\mathbf{F}\mathbf{Q}]^+$.

E Dataset Details

E.1 M4 Dataset Details

Table 3 outlines the composition of the M4 dataset across domains and forecast horizons by listing the number of TS

Table 3: Composition of the M4 dataset: the number of TS based on their sampling frequency and type.

Type	Frequency / Horizon						Total
	Yearly/6	Qtly/8	Monthly/18	Wkly/13	Daily/14	Hrly/48	
Demographic	1,088	1,858	5,728	24	10	0	8,708
Finance	6,519	5,305	10,987	164	1,559	0	24,534
Industry	3,716	4,637	10,017	6	422	0	18,798
Macro	3,903	5,315	10,016	41	127	0	19,402
Micro	6,538	6,020	10,975	112	1,476	0	25,121
Other	1,236	865	277	12	633	414	3,437
Total	23,000	24,000	48,000	359	4,227	414	100,000
Min. Length	19	24	60	93	107	748	
Max. Length	841	874	2812	2610	9933	1008	
Mean Length	37.3	100.2	234.3	1035.0	2371.4	901.9	
SD Length	24.5	51.1	137.4	707.1	1756.6	127.9	
% Smooth	82%	89%	94%	84%	98%	83%	
% Erratic	18%	11%	6%	16%	2%	17%	

based on their frequency and type (M4 Team 2018). The M4 dataset is large and diverse: all forecast horizons are composed of heterogeneous TS types (with exception of Hourly) frequently encountered in business, financial and economic forecasting. Summary statistics on series lengths are also listed, showing wide variability therein, as well as a characterization (*smooth vs erratic*) that follows Syntetos, Boylan, and Croston (2005), and is based on the squared coefficient of variation of the series. All series have positive observed values at all time-steps; as such, none can be considered *intermittent* or *lumpy* per Syntetos, Boylan, and Croston (2005).

E.2 FRED Dataset Details

FRED is a large-scale dataset introduced in this paper containing around 290k US and international economic TS from 89 sources, a subset of Federal Reserve economic data (Federal Reserve 2019). FRED is downloaded using a custom download script based on the high-level FRED python API (Velkoski 2016). This is a python wrapper over the low-level web-based FRED API. For each point in a time-series the raw data published at the time of first release are downloaded. All time series with any NaN entries have been filtered out. We focus our attention on Yearly, Quarterly, Monthly, Weekly and Daily frequency data. Other frequencies are available, for example, bi-weekly and five-yearly. They are skipped, because only being present in small quantities. These factors explain the fact that the size of the dataset we assembled for this study is 290k, while 672k total time-series are in principle available (Federal Reserve 2019). Hourly data are not available in this dataset. For the data frequencies included in FRED dataset, we use the same forecasting horizons as for the M4 dataset: Yearly: 6, Quarterly: 8, Monthly: 18, Weekly: 13 and Daily: 14. The dataset download takes approximately 7–10 days, because of the bandwidth constraints imposed by the low-level FRED API. The test, validation and train subsets are defined in the usual way. The test set is derived by splitting the full FRED dataset at the left boundary of the last horizon of each time series.

Similarly, the validation set is derived from the penultimate horizon of each time series.

E.3 M3 Dataset Details

Table 4 outlines the composition of the M3 dataset across domains and forecast horizons by listing the number of TS based on their frequency and type (Makridakis and Hibon 2000). The M3 is smaller than the M4, but it is still large and diverse: all forecast horizons are composed of heterogeneous TS types frequently encountered in business, financial and economic forecasting. Over the past 20 years, this dataset has supported significant efforts in the design of advanced statistical models, e.g. Theta and its variants (Assimakopoulos and Nikolopoulos 2000; Fiorucci et al. 2016; Spiliotis, Assimakopoulos, and Nikolopoulos 2019). Summary statistics on series lengths are also listed, showing wide variability in length, as well as a characterization (*smooth vs erratic*) that follows Syntetos, Boylan, and Croston (2005), and is based on the squared coefficient of variation of the series. All series have positive observed values at all time-steps; as such, none can be considered *intermittent* or *lumpy* per Syntetos, Boylan, and Croston (2005).

E.4 TOURISM Dataset Details

Table 5 outlines the composition of the TOURISM dataset across forecast horizons by listing the number of TS based on their frequency. Summary statistics on series lengths are listed, showing wide variability in length. All series have positive observed values at all time-steps. In contrast to M4 and M3 datasets, TOURISM includes a much higher fraction of erratic series.

Table 4: Composition of the M3 dataset: the number of TS based on their sampling frequency and type.

Type	Frequency / Horizon				Total
	Yearly/6	Quarterly/8	Monthly/18	Other/8	
Demographic	245	57	111	0	413
Finance	58	76	145	29	308
Industry	102	83	334	0	519
Macro	83	336	312	0	731
Micro	146	204	474	4	828
Other	11	0	52	141	204
Total	645	756	1,428	174	3,003
Min. Length	20	24	66	71	
Max. Length	47	72	144	104	
Mean Length	28.4	48.9	117.3	76.6	
SD Length	9.9	10.6	28.5	10.9	
% Smooth	90%	99%	98%	100%	
% Erratic	10%	1%	2%	0%	

Table 5: Composition of the TOURISM dataset: the number of TS based on their sampling frequency.

	Frequency / Horizon			Total
	Yearly/4	Quarterly/8	Monthly/24	
	518	427	366	1,311
Min. Length	11	30	91	
Max. Length	47	130	333	
Mean Length	24.4	99.6	298	
SD Length	5.5	20.3	55.7	
% Smooth	77%	61%	49%	
% Erratic	23%	39%	51%	

E.5 ELECTRICITY and TRAFFIC Dataset Details

ELECTRICITY² and TRAFFIC³ datasets (Dua and Graff 2017; Yu, Rao, and Dhillon 2016) are both part of UCI repository. ELECTRICITY represents the hourly electricity usage monitoring of 370 customers over three years. TRAFFIC dataset tracks the hourly occupancy rates scaled in (0,1) range of 963 lanes in the San Francisco bay area freeways over a period of slightly more than a year. Both datasets exhibit strong hourly and daily seasonality patterns.

Both datasets are aggregated to hourly data, but using different aggregation operations: sum for ELECTRICITY and mean for TRAFFIC. The hourly aggregation is done so that all the points available in $(h - 1 : 00, h : 00]$ hours are aggregated to hour h , thus if original dataset starts on 2011-01-01 00:15 then the first time point after aggregation will be 2011-01-01 01:00. For the ELECTRICITY dataset we removed the first year from training set, to match the training set used in (Yu, Rao, and Dhillon 2016), based on the aggregated dataset downloaded from, presumable authors’, Github repository⁴.

²<https://archive.ics.uci.edu/ml/datasets/ElectricityLoadDiagrams20112014>

³<https://archive.ics.uci.edu/ml/datasets/PEMS-SF>

⁴<https://github.com/rofuyu/exp-trmf-nips16/blob/master/>

We also made sure that data points for both ELECTRICITY and TRAFFIC datasets after aggregation match those used in (Yu, Rao, and Dhillon 2016). The authors of the Mat-Fact model were using the last 7 days of datasets as test set, but papers from Amazon DeepAR (Flunkert, Salinas, and Gasthaus 2017), Deep State (Rangapuram et al. 2018), Deep Factors (Wang et al. 2019) are using different splits, where the split points are provided by a date. Changing split points without a well-grounded reason adds uncertainties to the comparability of the models performances and creates challenges to the reproducibility of the results, thus we were trying to match all different splits in our experiments. It was especially challenging on TRAFFIC dataset, where we had to use some heuristics to find records dates; the dataset authors state: “The measurements cover the period from Jan. 1st 2008 to Mar. 30th 2009” and “We remove public holidays from the dataset, as well as two days with anomalies (March 8th 2009 and March 9th 2008) where all sensors were muted between 2:00 and 3:00 AM.” In spite of this, we failed to match a part of the provided labels of week days to actual dates. Therefore, we had to assume that the actual list of gaps, which include holidays and anomalous days, is as follows:

1. Jan. 1, 2008 (New Year’s Day)
2. Jan. 21, 2008 (Martin Luther King Jr. Day)
3. Feb. 18, 2008 (Washington’s Birthday)
4. Mar. 9, 2008 (Anomaly day)
5. May 26, 2008 (Memorial Day)
6. Jul. 4, 2008 (Independence Day)
7. Sep. 1, 2008 (Labor Day)
8. Oct. 13, 2008 (Columbus Day)
9. Nov. 11, 2008 (Veterans Day)
10. Nov. 27, 2008 (Thanksgiving)
11. Dec. 25, 2008 (Christmas Day)

[python/exp-scripts/datasets/download-data.sh](https://github.com/rofuyu/exp-trmf-nips16/blob/master/python/exp-scripts/datasets/download-data.sh)

12. Jan. 1, 2009 (New Year’s Day)
13. Jan. 19, 2009 (Martin Luther King Jr. Day)
14. Feb. 16, 2009 (Washington’s Birthday)
15. Mar. 8, 2009 (Anomaly day)

The first six gaps were confirmed by the gaps in labels, but the rest were more than one day apart from any public holiday of years 2008 and 2009 in San Francisco, California and US. Moreover, the number of gaps we found in the labels provided by dataset authors is 10, while the number of days between Jan. 1st 2008 and Mar. 30th 2009 is 455, assuming that Jan. 1st 2008 was skipped from the values and labels we should end up with either $454 - 10 = 444$ instead of 440 days or different end date. The metric used to evaluate performance on the datasets is ND (Yu, Rao, and Dhillon 2016), which is equal to $p50$ loss used in DeepAR, Deep State, and Deep Factors papers.

E.6 Overlaps Between Datasets

Some of the datasets used in experiments consist of time series from different domains. Thus, it would be reasonable to suggest that the target dataset, used for transfer learning performance evaluation, could contain time series from the source dataset. To validate that the model performance is not affected by the fact that these datasets may share parts of time series we have performed sequence to sequence comparison between training and testing sets. The searched sequence is constructed from the last horizon of the input, provided to model during test, and the test part of the target dataset, forming the chunks of two horizons length. Then the searched sequence is compared to every sequence of the source dataset. This method allows to spot training cases where the last part of the input with the output have exact match with the last two horizons of time series from the target dataset, used for performance evaluation. We have found that the only datasets which have common sequences are M4 and FRED: 3 in Yearly, 34 in Quarterly and 195 in Monthly. Taking into account the total number of time series in these datasets, the effect from overlap can be considered as insignificant.

F Empirical Results Details

On all datasets, we consider the original N-BEATS (Oreshkin et al. 2020), the model trained on a given dataset and applied to this same dataset. This is provided for the purpose of assessing the generalization gap of the zero-shot N-BEATS. We consider four variants of zero-shot N-BEATS: NB-SH-M4, NB-NSH-M4, NB-SH-FR, NB-NSH-FR. -SH/-NSH option signifies block weight sharing ON/OFF. -M4/-FR option signifies M4/FRED source dataset. The mapping between seasonal patterns of target and source datasets is presented in Table 6. The model architecture and training procedure does not depend on the source dataset, i.e. we used the same parameters to train models from M4 and FRED. The parameters values can be found in Table 7. The results are calculated based on ensembles of 90 models: 6 lookback horizons, 3 loss functions, and 5 repeats. Models were trained using the training parts of the source datasets.

Table 6: Mapping of seasonal patterns between source and target datasets. †Monthly dataset was linearly interpolated to match hourly period.

	M4	FRED
FRED		
Yearly	Yearly	–
Quarterly	Quarterly	–
Monthly	Monthly	–
Weekly	Weekly	–
Daily	Daily	–
M4		
Yearly	–	Yearly
Quarterly	–	Quarterly
Monthly	–	Monthly
Weekly	–	Monthly
Daily	–	Monthly
Hourly	–	Monthly [†]
M3		
Yearly	Yearly	Yearly
Quarterly	Quarterly	Quarterly
Monthly	Monthly	Monthly
Others	Quarterly	Quarterly
TOURISM		
Yearly	Yearly	Yearly
Quarterly	Quarterly	Quarterly
Monthly	Monthly	Monthly
ELECTRICITY		
Hourly	Hourly	Monthly [†]
TRAFFIC		
Hourly	Hourly	Monthly [†]

F.1 Detailed M4 Results

On M4 we compare against five M4 competition entries, each representative of a broad model class. Best pure ML is the submission by B. Trotta, the best entry among the 6 pure ML models. Best statistical is the best pure statistical model by N.Z. Legaki and K. Koutsouri. ProLogistica is a weighted ensemble of statistical methods, the third best M4 participant. Best ML/TS combination is the model by (Montero-Manso et al. 2020), second best entry, gradient boosted tree over a few statistical time series models. Finally, *DL/TS hybrid* is the winner of M4 competition (Smyl 2020). Results are presented in Table 8.

F.2 Detailed FRED Results

We compare against well established off-the-shelf statistical models available from the R *forecast* package (Hyndman and Khandakar 2008). Those include Naïve (repeating the last value), ARIMA, Theta, SES and ETS. The quality metric is the regular sMAPE defined in (1).

F.3 Detailed M3 Results

We used the original M3 sMAPE metric to be able to compare against the results published in the literature. The sMAPE used for M3 is different from the metric defined in (1) in that it does not have the absolute values of the values in the

Table 7: Model parameters

Source Datasets	M4, FRED
Loss Functions	MASE, MAPE, SMAPE
Number of Blocks	30
Layers in Block	4
Layer Size	512
Iterations	15 000
Lookback Horizons	2, 3, 4, 5, 6, 7
History size	10 horizons
Learning rate	10^{-3}
Batch size	1024
Repeats	5

denominator:

$$\text{SMAPE} = \frac{200}{H} \sum_{i=1}^H \frac{|y_{T+i} - \hat{y}_{T+i}|}{y_{T+i} + \hat{y}_{T+i}}. \quad (11)$$

The detailed zero-shot transfer results on M3 from FRED and M4 are presented in Table 10.

On M3 dataset (Makridakis and Hibon 2000), we compare against the *Theta* method (Assimakopoulos and Nikolopoulos 2000), the winner of M3; *DOTA*, a dynamically optimized Theta model (Fiorucci et al. 2016); *EXP*, the most recent statistical approach and the previous state-of-the-art on M3 (Spiliotis, Assimakopoulos, and Nikolopoulos 2019); as well as *ForecastPro*, an off-the-shelf forecasting software that is based on model selection between exponential smoothing, ARIMA and moving average (Athanasopoulos et al. 2011; Assimakopoulos and Nikolopoulos 2000). We also include the DeepAR model trained on M3, denoted ‘DeepAR’, as well as DeepAR trained on M4 and tested in zero-shot transfer mode on M3, denoted ‘DeepAR-M4’. Please see (Makridakis and Hibon 2000) for the details of other models.

F.4 Detailed TOURISM Results

On the TOURISM dataset (Athanasopoulos et al. 2011), we compare against three statistical benchmarks: *ETS*, exponential smoothing with cross-validated additive/multiplicative model; *Theta* method; *ForePro*, same as *ForecastPro* in M3; as well as top 2 entries from the TOURISM Kaggle competition (Athanasopoulos and Hyndman 2011): *Stratometrics*, an unknown technique; *LeeCBaker* (Baker and Howard 2011), a weighted combination of Naïve, linear trend model, and exponentially weighted least squares regression trend. We also include the DeepAR model trained on TOURISM, denoted ‘DeepAR’, as well as DeepAR trained on M4 and tested in zero-shot transfer mode on TOURISM, denoted ‘DeepAR-M4’. Please see (Athanasopoulos et al. 2011) for the details of other models.

F.5 Detailed ELECTRICITY Results

On ELECTRICITY, we compare against MatFact (Yu, Rao, and Dhillon 2016), DeepAR (Flunkert, Salinas, and Gasthaus 2017), Deep State (Rangapuram et al. 2018), Deep Factors (Wang et al. 2019). We use ND metric that was used in those papers. The results are presented in in Table 12. We present our results on 3 different splits, as explained in Appendix E.5.

F.6 Detailed TRAFFIC Results

On TRAFFIC, we compare against MatFact (Yu, Rao, and Dhillon 2016), DeepAR (Flunkert, Salinas, and Gasthaus 2017), Deep State (Rangapuram et al. 2018), Deep Factors (Wang et al. 2019). We use ND metric that was used in those papers. The results are presented in in Table 13. We present our results on 3 different splits, as explained in Appendix E.5.

G The Details of the Study of Meta-learning Effects

Figures 3 and 4 detail the performance across a number of datasets, as the number of N-BEATS blocks is varied. Illustrated on the plots are the effects of having the same parameters being shared across all blocks (blue curves) or having individual parameters (red curves).

Table 8: Performance on the M4 test set, SMAPE. Lower values are better. *DeepAR trained by us using GluonTS.

	Yearly (23k)	Quarterly (24k)	Monthly (48k)	Others (5k)	Average (100k)
Best pure ML	14.397	11.031	13.973	4.566	12.894
Best statistical	13.366	10.155	13.002	4.682	11.986
ProLogistica	13.943	9.796	12.747	3.365	11.845
Best ML/TS combination	13.528	9.733	12.639	4.118	11.720
DL/TS hybrid, M4 winner	13.176	9.679	12.126	4.014	11.374
DeepAR*	12.362	10.822	13.705	4.668	12.253
N-BEATS	12.913	9.213	12.024	3.643	11.135
NB-SH-FR	13.267	9.634	12.694	4.892	11.701
NB-NSH-FR	13.272	9.596	12.676	4.696	11.675

Table 9: Performance on the FRED test set, SMAPE. Lower values are better.

	Yearly (133,554)	Quarterly (57,569)	Monthly (99,558)	Weekly (1,348)	Daily (17)	Average (292,046)
Theta	16.50	14.24	5.35	6.29	10.57	12.20
ARIMA	16.21	14.25	5.58	5.51	9.88	12.15
SES	16.61	14.58	6.45	5.38	7.75	12.70
ETS	16.46	19.34	8.18	5.44	8.07	14.52
Naïve	16.59	14.86	6.59	5.41	8.65	12.79
N-BEATS	15.79	13.27	4.79	4.63	8.86	11.49
NB-SH-M4	15.00	13.36	6.10	5.67	8.57	11.60
NB-NSH-M4	15.06	13.48	6.24	5.71	9.21	11.70

Table 10: M3 SMAPE defined in (11). †Numbers from Appendix C.2, Detailed results: M3 Dataset, of (Oreshkin et al. 2020). *DeepAR trained by us using GluonTS.

	Yearly (645)	Quarterly (756)	Monthly (1428)	Others (174)	Average (3003)
Naïve2	17.88	9.95	16.91	6.30	15.47
ARIMA (B–J automatic)	17.73	10.26	14.81	5.06	14.01
Comb S-H-D	17.07	9.22	14.48	4.56	13.52
ForecastPro	17.14	9.77	13.86	4.60	13.19
Theta	16.90	8.96	13.85	4.41	13.01
DOTM (Fiorucci et al. 2016)	15.94	9.28	13.74	4.58	12.90
EXP (Spiliotis, Assimakopoulos, and Nikolopoulos 2019)	16.39	8.98	13.43	5.46	12.71 [†]
LGT (Smyl and Kuber 2016)	15.23	n/a	n/a	4.26	n/a
BaggedETS.BC (Bergmeir, Hyndman, and Benítez 2016)	17.49	9.89	13.74	n/a	n/a
DeepAR*	13.33	9.07	13.72	7.11	12.67
N-BEATS	15.93	8.84	13.11	4.24	12.37
NB-SH-M4	15.25	9.07	13.25	4.34	12.44
NB-NSH-M4	15.07	9.10	13.19	4.29	12.38
NB-SH-FR	16.43	9.05	13.42	4.67	12.69
NB-NSH-FR	16.48	9.07	13.30	4.51	12.61
DeepAR-M4*	14.76	9.28	16.15	13.09	14.76

Table 11: TOURISM, MAPE. *DeepAR trained by us using GluonTS.

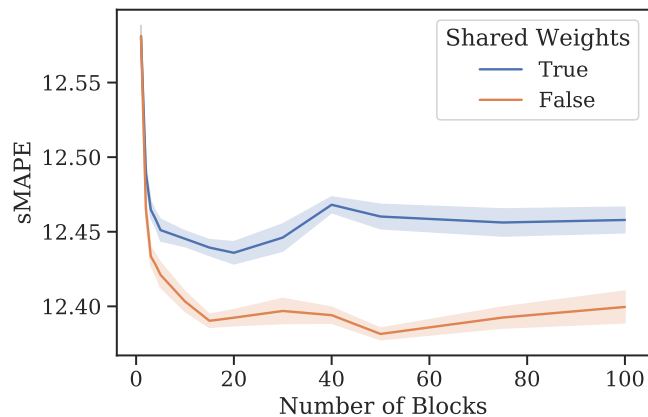
	Yearly (518)	Quarterly (427)	Monthly (366)	Average (1311)
Statistical benchmarks				
SNaïve	23.61	16.46	22.56	21.25
Theta	23.45	16.15	22.11	20.88
ForePro	26.36	15.72	19.91	19.84
ETS	27.68	16.05	21.15	20.88
Damped	28.15	15.56	23.47	22.26
ARIMA	28.03	16.23	21.13	20.96
Kaggle competitors				
SaliMali	n/a	14.83	19.64	n/a
LeeCBaker	22.73	15.14	20.19	19.35
Stratometrics	23.15	15.14	20.37	19.52
Robert	n/a	14.96	20.28	n/a
Idalgo	n/a	15.07	20.55	n/a
DeepAR*	21.14	15.82	20.18	19.27
N-BEATS	21.44	14.78	19.29	18.52
NB-SH-M4	23.57	14.66	19.33	18.82
NB-NSH-M4	24.04	14.78	19.32	18.92
NB-SH-FR	23.53	14.47	21.23	19.94
NB-NSH-FR	23.43	14.45	20.47	19.46
DeepAR-M4*	21.51	22.01	26.64	24.79

Table 12: ELECTRICITY, ND. †Numbers reported by Flunkert, Salinas, and Gasthaus (2017), different from the originally reported MatFact results, most probably due to changed split point. *DeepAR trained by us using GluonTS

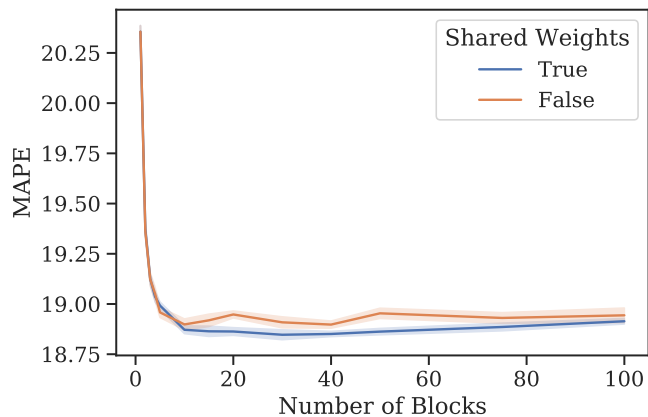
	2014-09-01 (DeepAR split)	2014-03-31 (Deep Factors split)	last 7 days (MatFact split)
MatFact	0.160 [†]	n/a	0.255
DeepAR	0.070	0.272	n/a
Deep State	0.083	n/a	n/a
Deep Factors	n/a	0.112	n/a
Theta	0.079	0.080	0.191
ARIMA	0.067	0.068	0.225
ETS	0.083	0.075	0.190
SES	0.372	0.320	0.365
DeepAR*	0.094	0.089	0.765
N-BEATS	0.067	0.067	0.178
NB-SH-M4	0.094	0.092	0.178
NB-NSH-M4	0.102	0.095	0.180
NB-SH-FR	0.091	0.084	0.205
NB-NSH-FR	0.085	0.080	0.207
DeepAR-M4*	0.151	0.081	0.532

Table 13: TRAFFIC, ND. †Numbers reported by Flunkert, Salinas, and Gasthaus (2017), different from the originally reported MatFact results, most probably due to changed split point. *DeepAR trained by us using GluonTS.

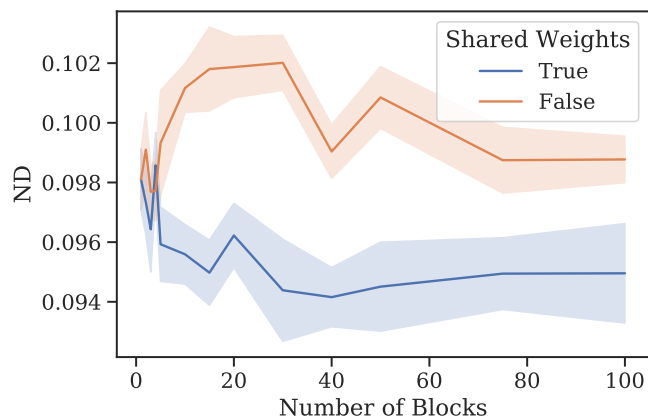
	2008-06-15 (DeepAR split)	2008-01-14 (Deep Factors split)	last 7 days (MatFact split)
MatFact	0.200 [†]	n/a	0.187
DeepAR	0.170	0.296	n/a
Deep State	0.167	n/a	n/a
Deep Factors	n/a	0.225	n/a
Theta	0.178	0.841	0.170
ARIMA	0.145	0.500	0.153
ETS	0.701	1.330	0.720
SES	0.634	1.110	0.637
DeepAR*	0.191	0.478	0.136
N-BEATS	0.114	0.230	0.111
NB-SH-M4	0.147	0.245	0.156
NB-NSH-M4	0.152	0.250	0.160
NB-SH-FR	0.260	0.355	0.265
NB-NSH-FR	0.259	0.348	0.265
DeepAR-M4*	0.355	0.410	0.363



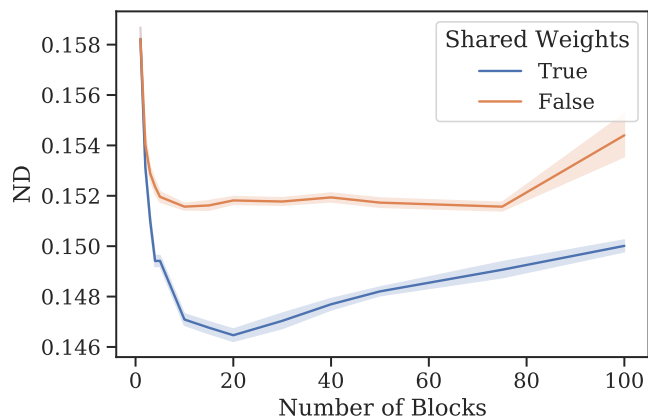
(a) M3



(b) Tourism

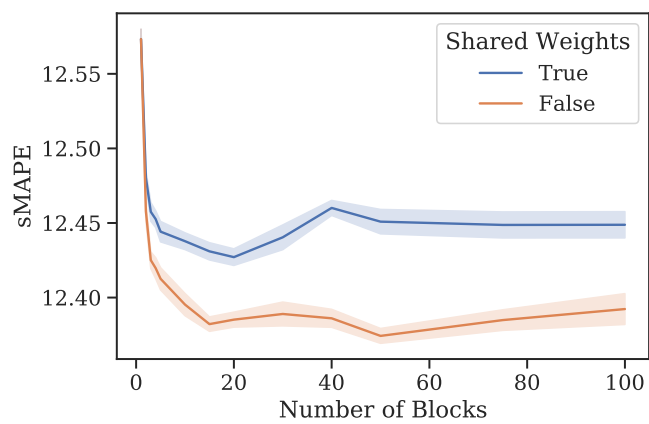


(c) Electricity

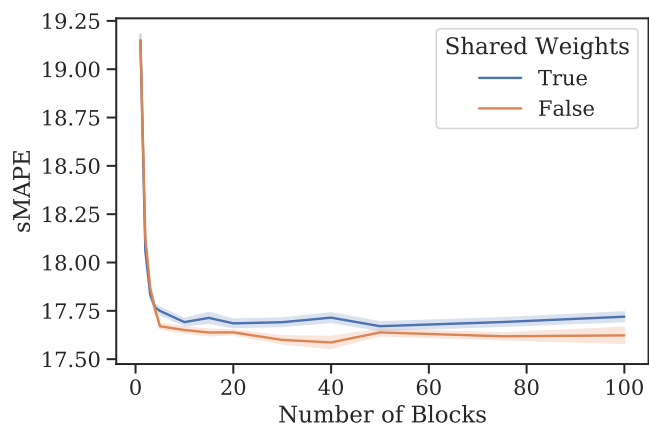


(d) Traffic

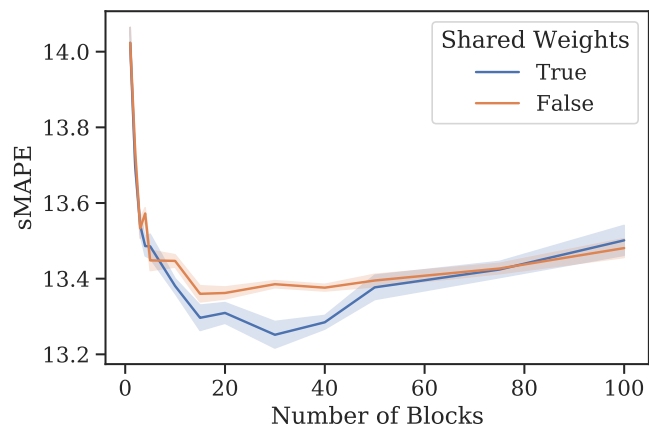
Figure 3: Evolution of performance metrics as a function of the number of N-BEATS blocks. Each plot combines metrics for both architectures with shared weights (blue line) and distinct weights (red line), respectively for M3, Tourism, Electricity, and Traffic. Each target dataset has its own performance metric, matching those in their respective literature. The results are based on ensemble of 30 models (5 different initializations with 6 different lookback periods), the mean and confidence interval (one standard deviation) are calculated based on performance of 30 different ensembles.



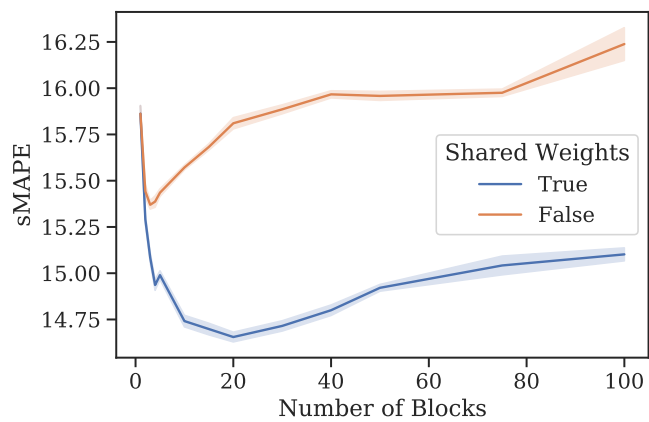
(a) M3



(b) Tourism



(c) Electricity



(d) Traffic

Figure 4: Same as Figure 3, but with unified metric sMAPE (1)